Grain Growth and Grain Growth Stagnation in Thin Films: Comparison of Experiments and Simulations

The Curious Tale of a Tail and an Ear

K. Barmak

Department of Applied Physics and
Applied Mathematics

COLUMBIA | ENGINEERING
The Fu Foundation School of Engineering and Applied Science

Acknowledge

- W. Archibald
- D. C. Carpenter
- A. Darbal
- C.-S. Kim
- J. Kim
- V. Kumar
- X. Liu
- T. Sun
- B. Yao
- J. Codner
- S. Roberts
- T. Shyu
- I. Livshits
- E. Eggeling
- R. Sharp
- D. Kinderlehrer
- A. D. Rollett
- G. S. Rohrer
- S. Ta'asan
- K. R. Coffey
- J. M. Rickman

MRSEC NSF DMR-0520425

SRC 1292.008 and 2121.001

Outline

- Introduction
- Experiments
- Simulations
- Comparison of Experiments and Simulations
- Summary and Conclusions

Example Applications of Thin Films

- Integrated circuits
- Hard disk drives

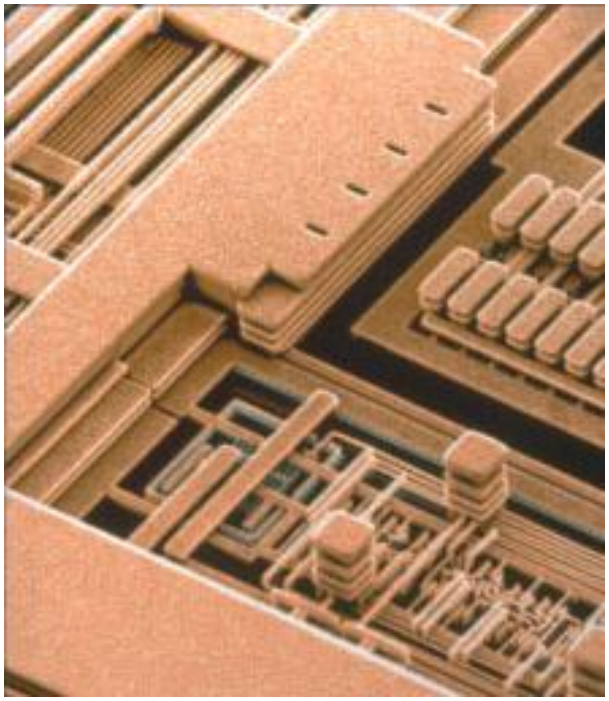

IBM CMOS 7S
ASIC with 6 levels of Cu

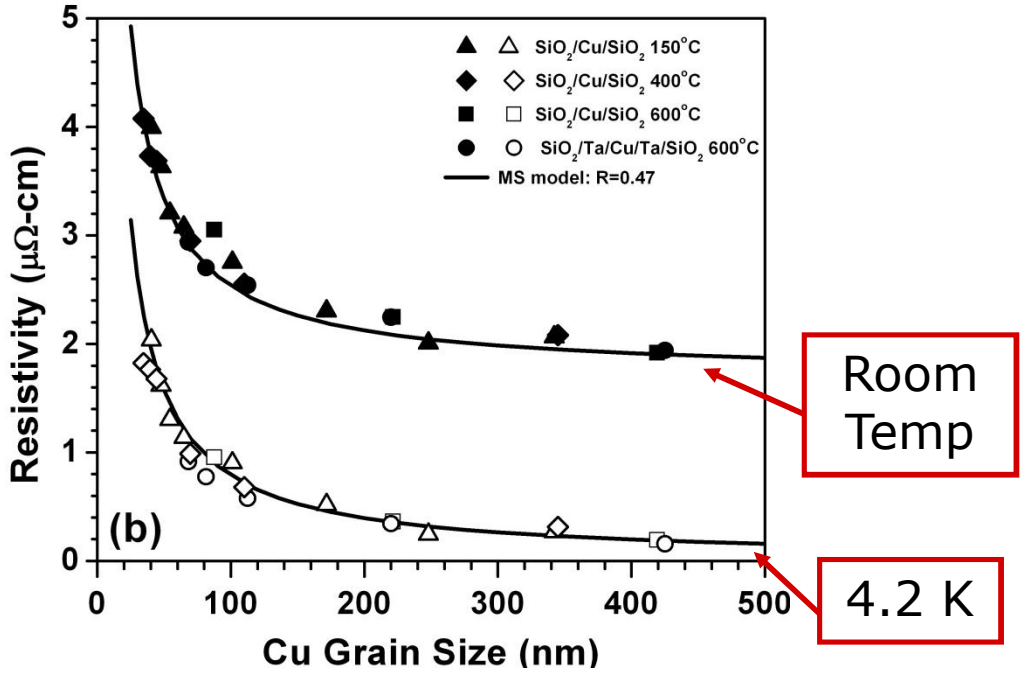

J. J. Thomson, Proc. Cambridge Philos. Soc. ***11****, 120 (1901).*

Sun et al., PRB ***81,*** *155454 (2010).*

Thin Films, Grain Structure and Grain Growth

UHV sputtering system

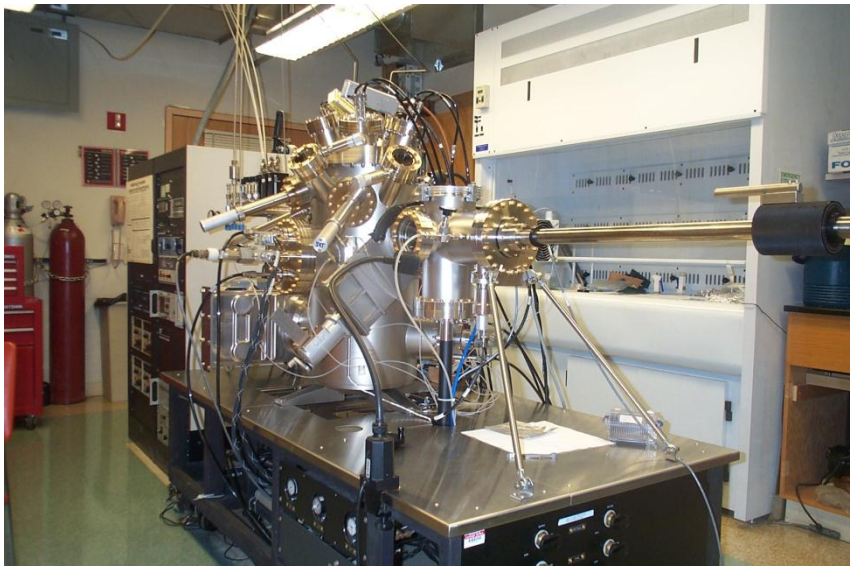

Diffraction pattern 2h, 18^{o} tilt

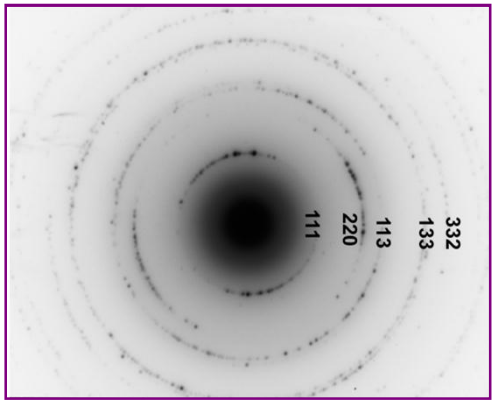

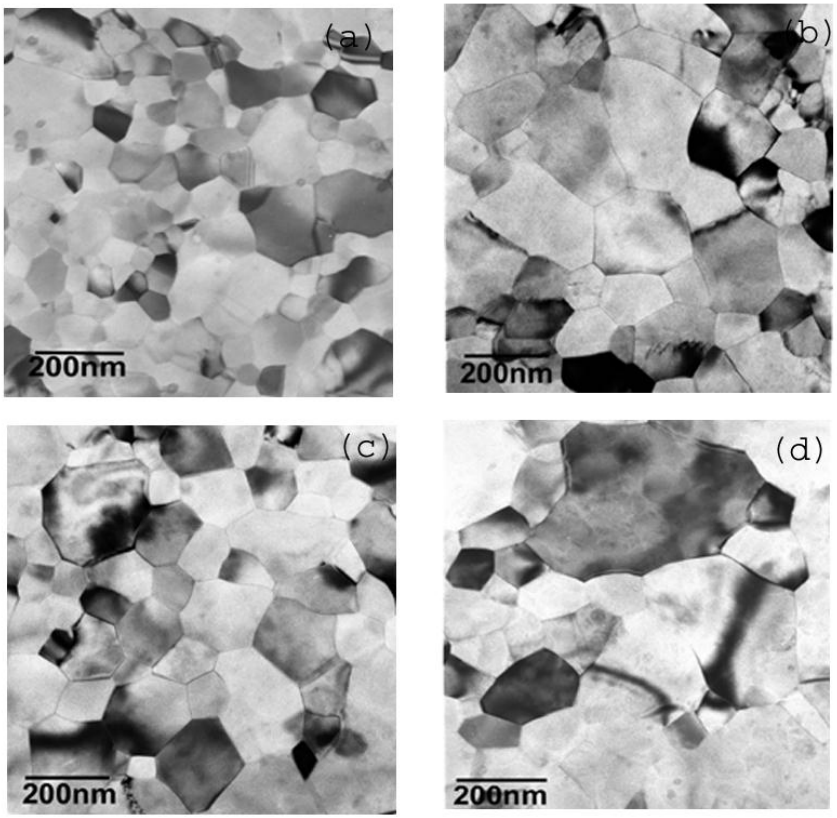

Bright-field transmission electron micrographs of 100 nm-thick Al films: (a) as-deposited, and annealed at 400 °C for (b) 2, (c) 4 and (d) 10 h.

Grain Structure: Cu and Al

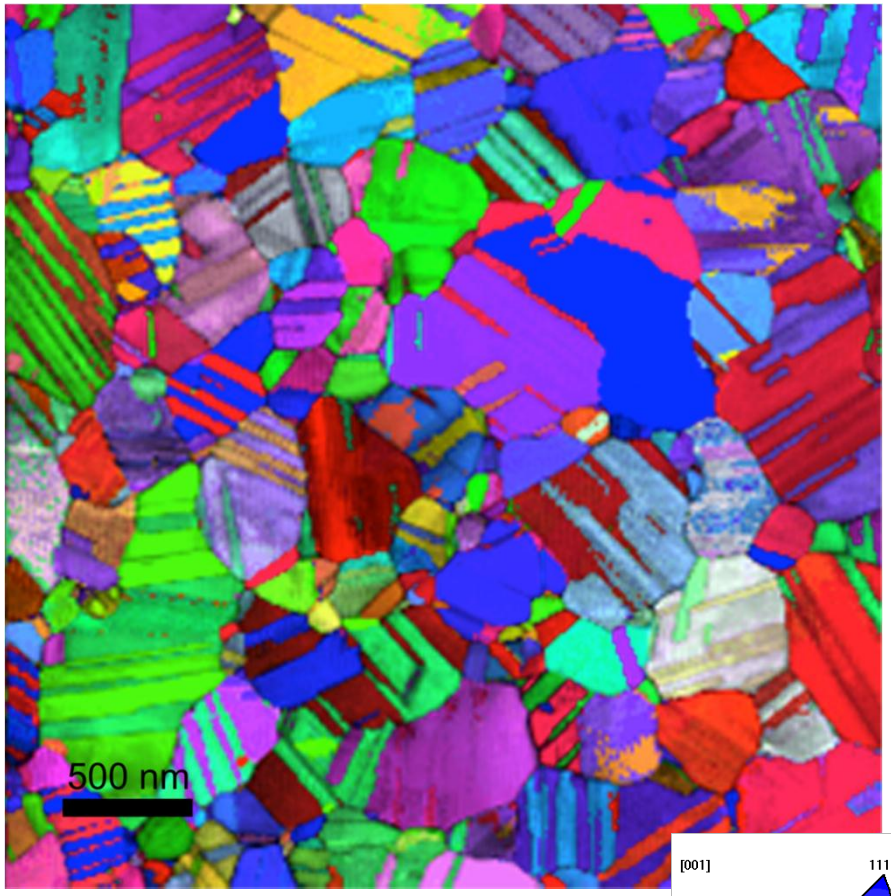

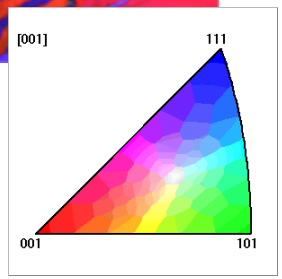

$Cu/Ta_{38}Si_{14}N_{48}$

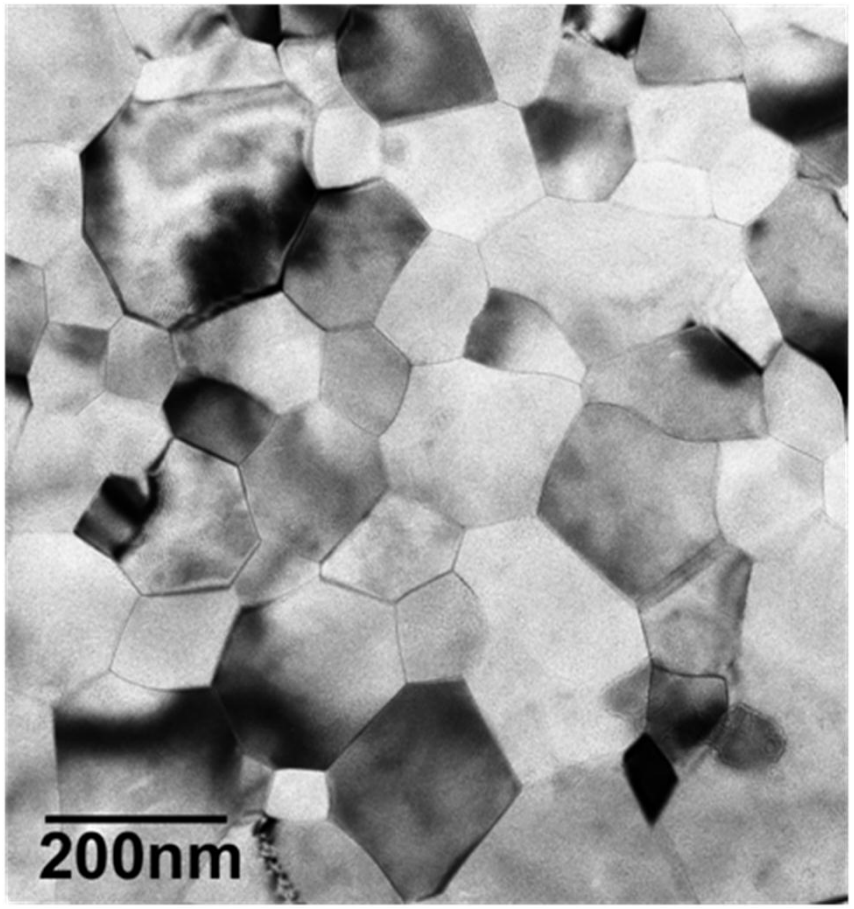

Al

Outline

- Introduction
- Experiments
- Simulations
- Comparison of Experiments and Simulations
- Summary and Conclusions

Experimental Data: Collection

Semi-automated

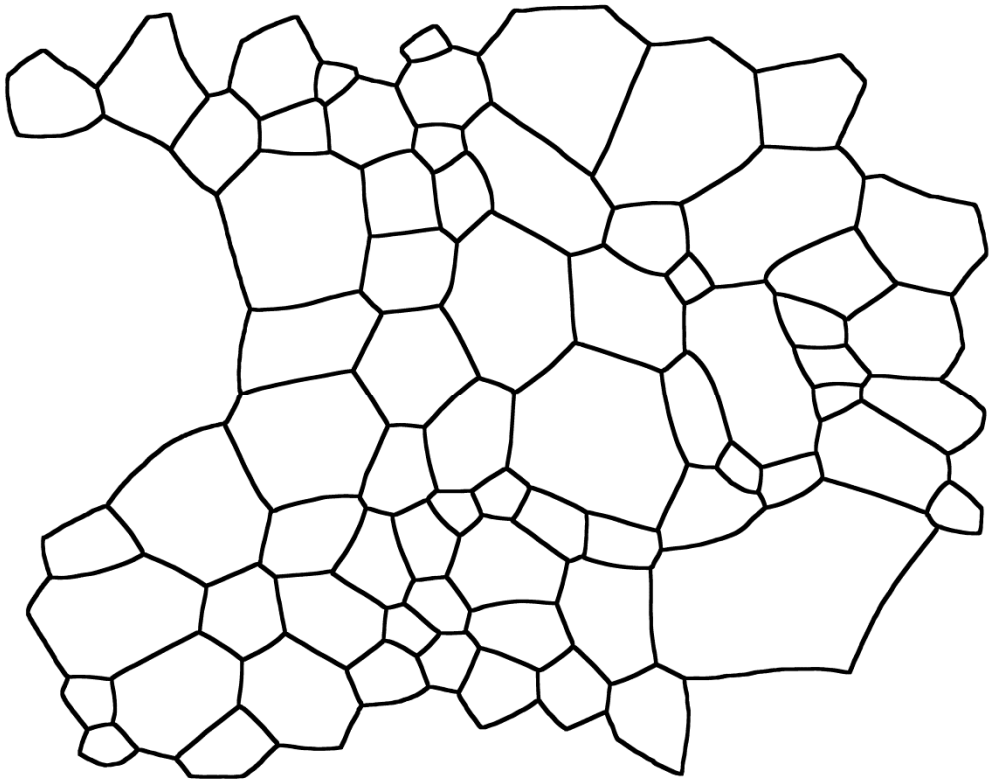

Use 2-4 images at different sample tilts.

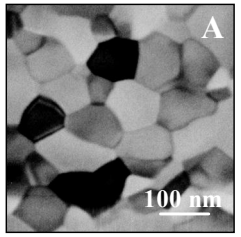

Automated

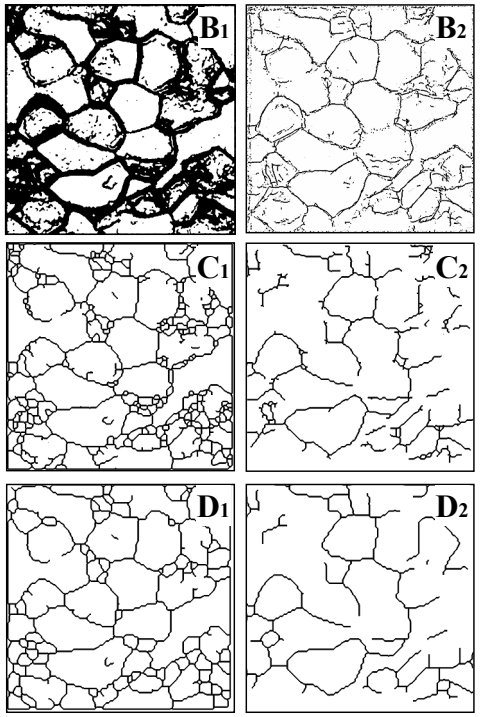

D. T. Carpenter, J. M. Rickman, K. Barmak, J. Appl. Phys. ***84****, 5843 (1998).*

Experimental Data Collection

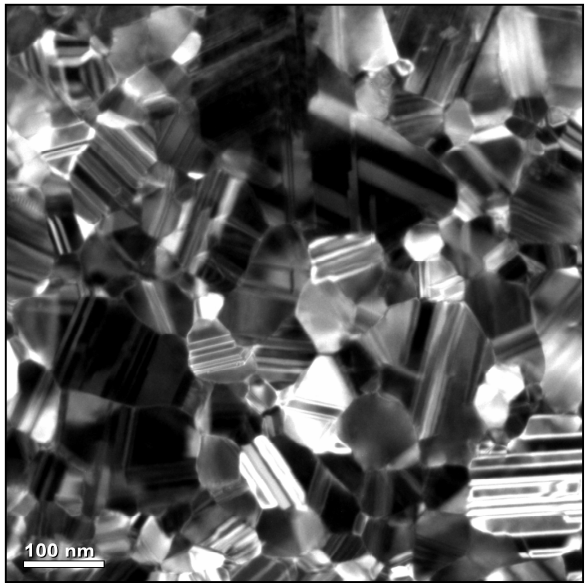

-2 degree tilt

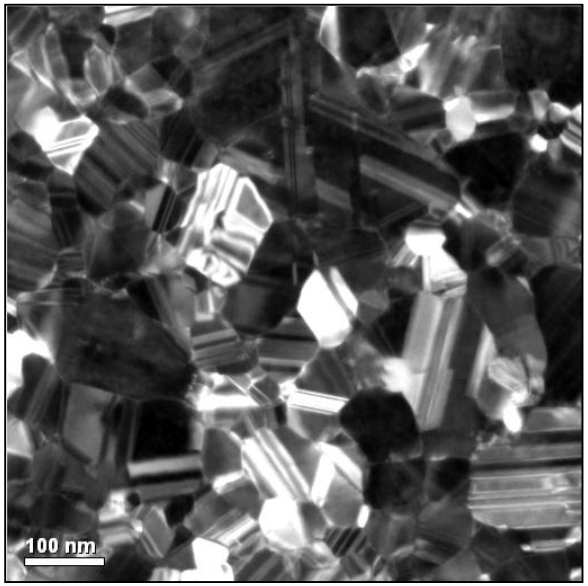

0 degree tilt

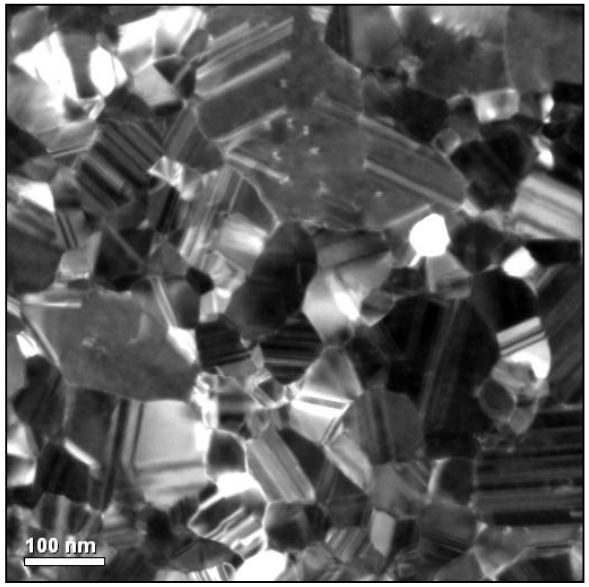

+2 degree tilt

The Cu 111, 200, 220, 311, and 222 reflections were used to form high contrast hollow cone dark field TEM images.

Experimental Data Collection

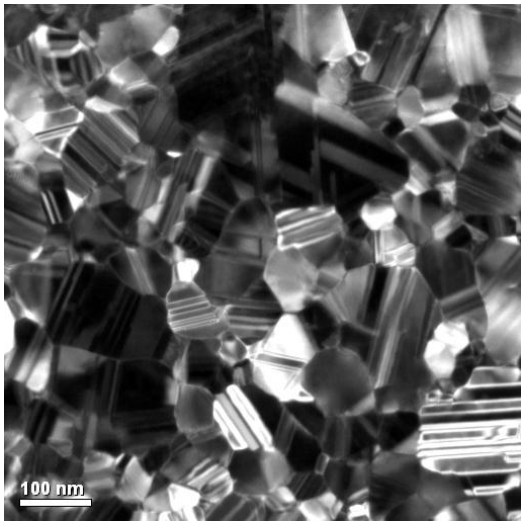

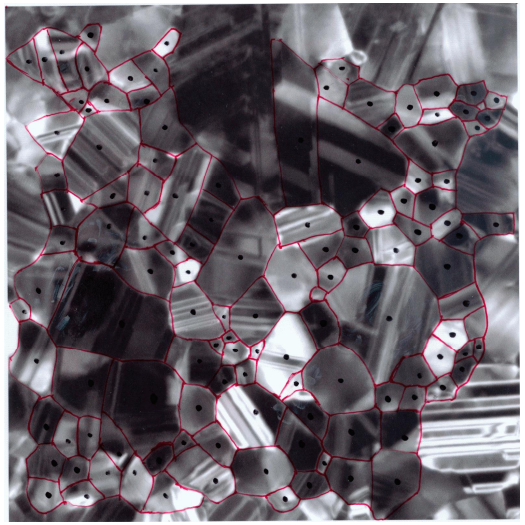

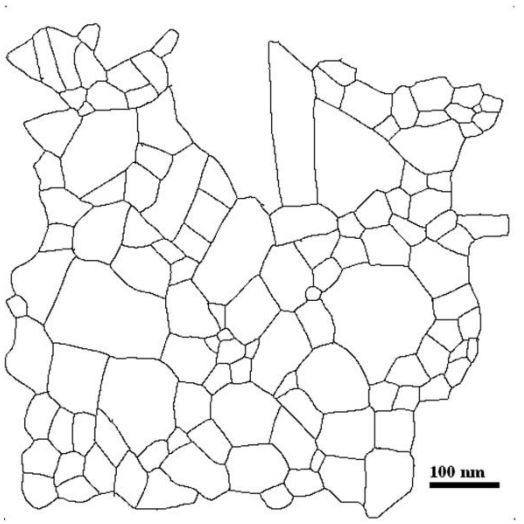

Semi-automated. Twin boundaries ignored.

Experimental Data Collection

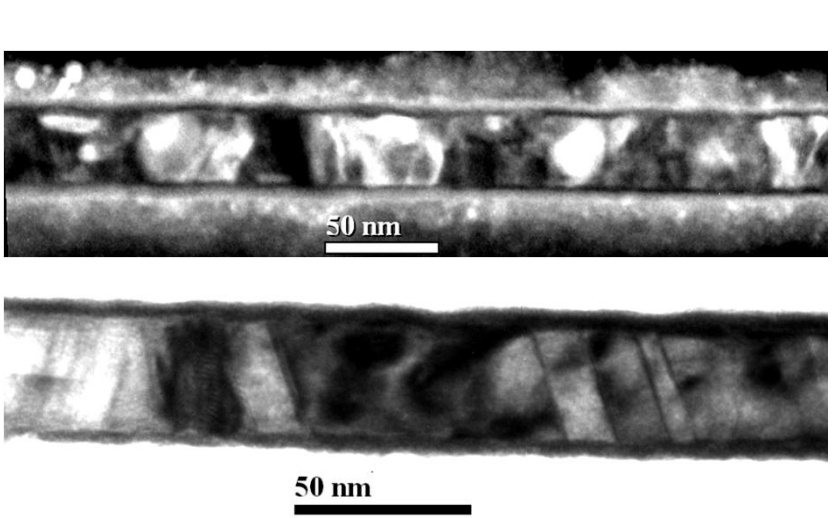

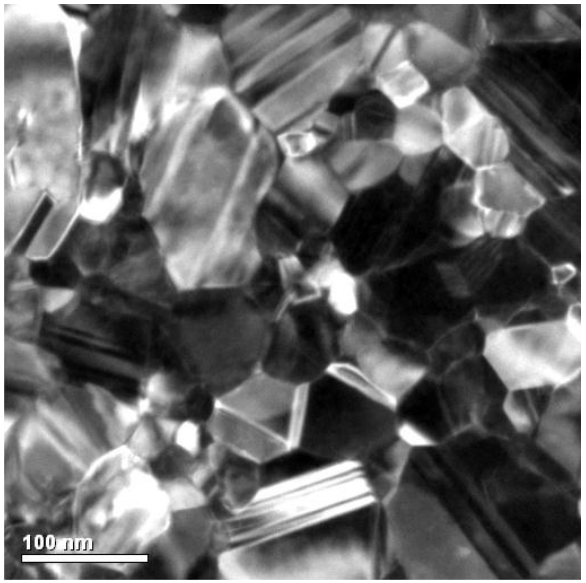

600 °C-annealed, Ta/SiO_2-capped, 40 nm-thick Cu film. Single grain through thickness.

Grain structure is columnar.

Experimental Data Collection

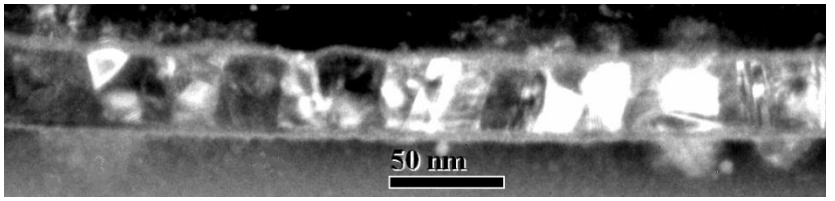

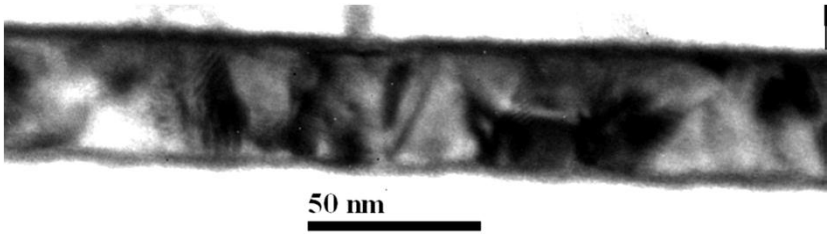

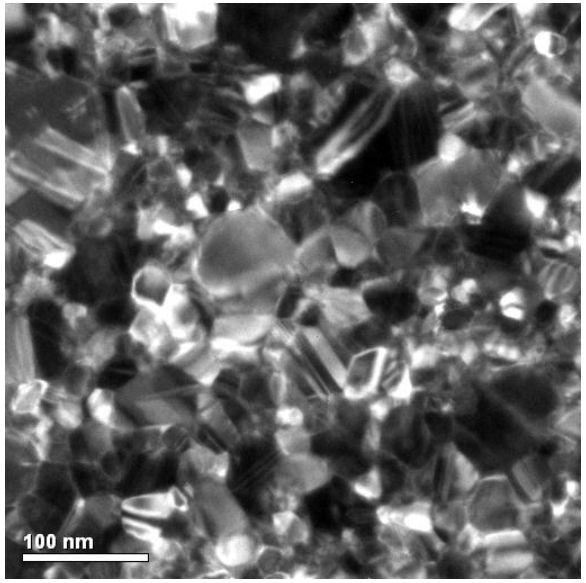

150 °C-annealed, Ta/SiO_2-capped, 40 nm-thick Cu film. Multiple grains through thickness. Samples not used.

Sides and Side Class of Neighbors

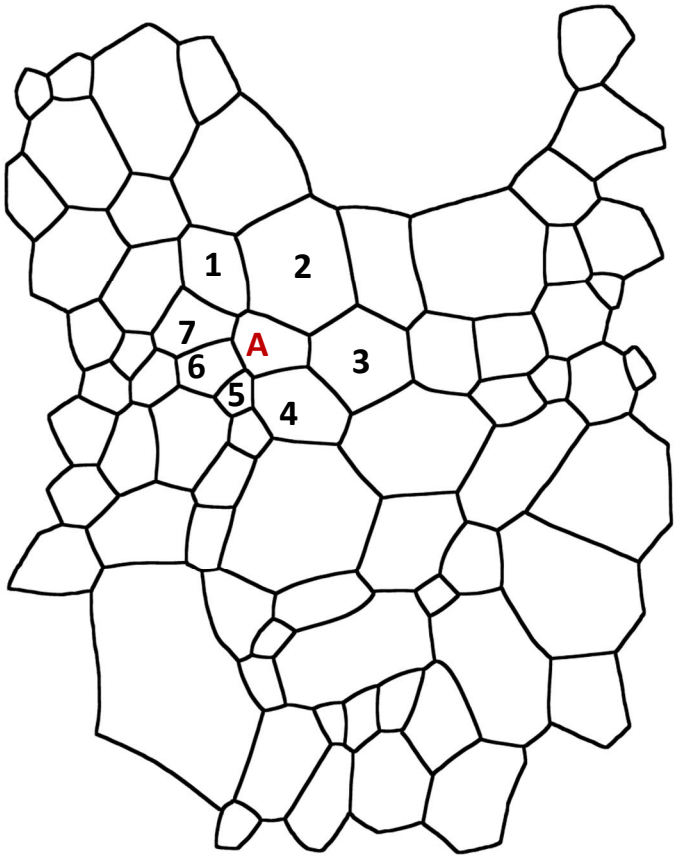

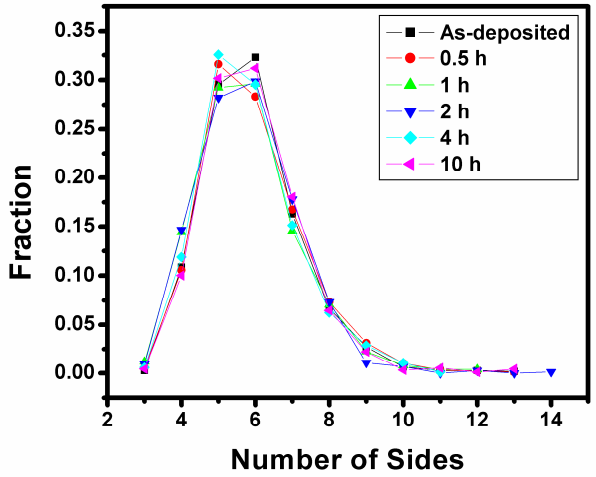

Annealing time at 400 °C (h)	Avg. no. of sides	No. of grains measured
0	5.9	1069
0.5	5.9	861
1	5.8	749
2	5.8	737
4	5.8	833
10	5.9	898

Minimum: 3

Maximum: 11-16

Most Frequent: 5, 6

Expected mean: 6

Grain Growth: Al

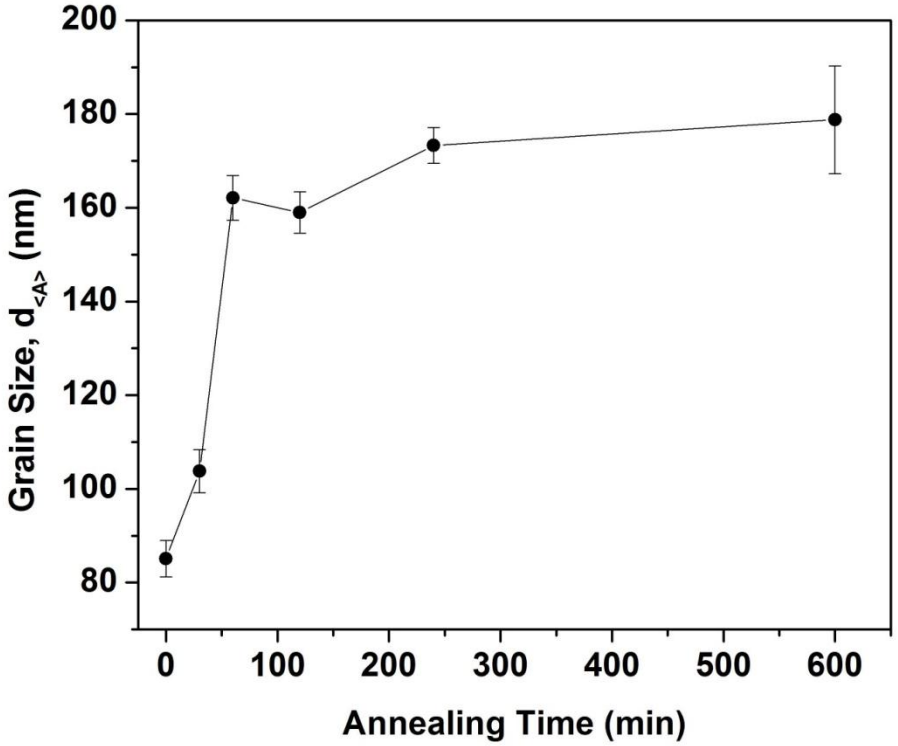

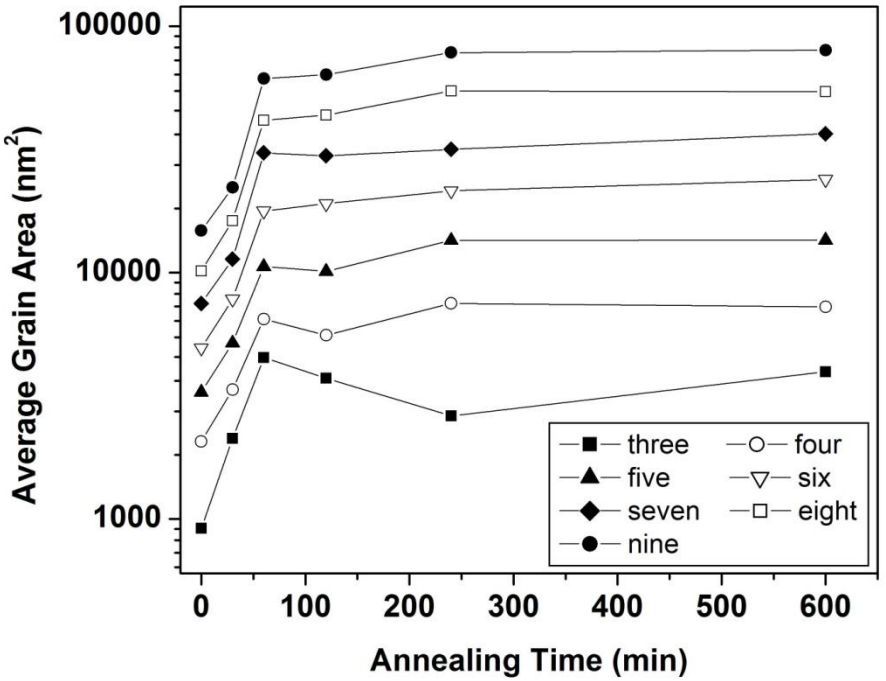

Grain growth stagnates, not just overall, but for every side class.

Grain Size Distribution: Al and Cu

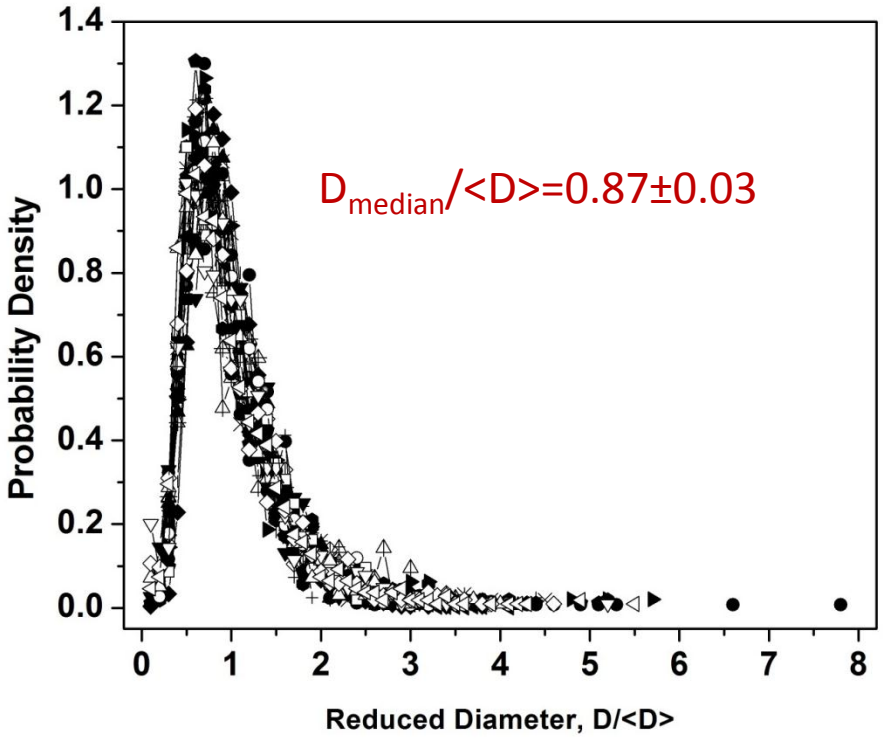

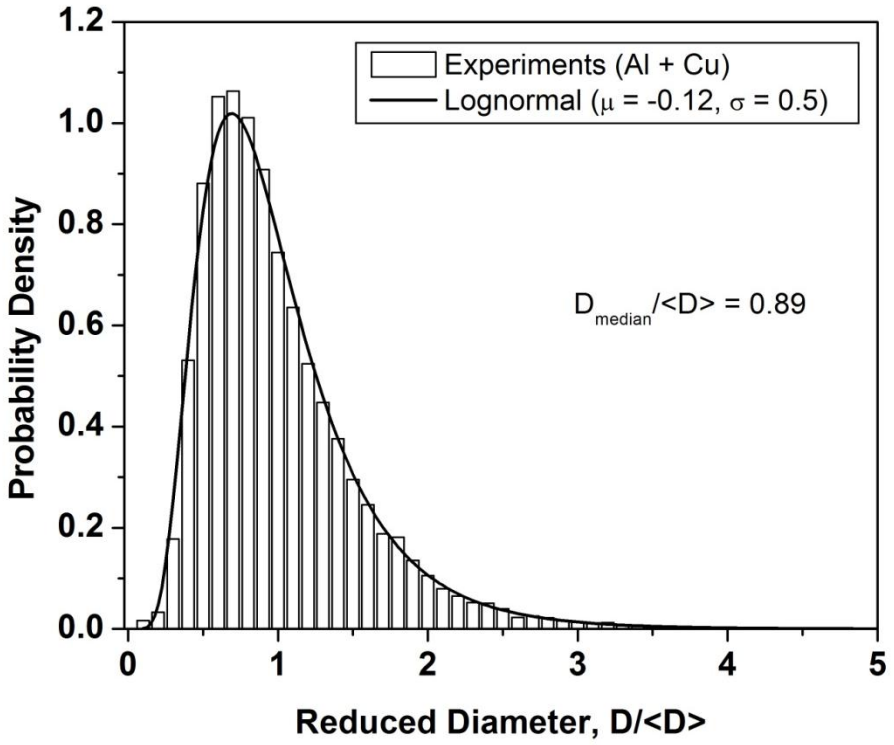

Data from 25 samples, 412-8185 grains per sample, for a total of 31,514 grains.

Remarks on the Experimental Results

- The size distributions for the Al and Cu films are remarkably similar to each other despite the many and significant differences in experimental conditions, which include:
  - Sputtering target purity (Al 99.9%, Cu 99.9999%)
  - Substrate type (SiO_2, $Ta_{38}Si_{14}N_{48}/SiO_2$, single crystal salt)
  - Film thickness (27-158 nm, factor of 5)
  - Deposition temperature, (room temperature for Al, vs. -40 °C for Cu)
  - Actual as well as homologous annealing temperatures (150-600 °C, 0.32-0.77)
  - Annealing time (6 s to 10 h)
  - Absolute grain size (40-425 nm)
  - Twin density within the grains (Al no twinning, Cu heavily twinned)

Outline

- Introduction
- Experiments
- Simulations
- Comparison of Experiments and Simulations
- Summary and Conclusions

Grain Growth Simulation

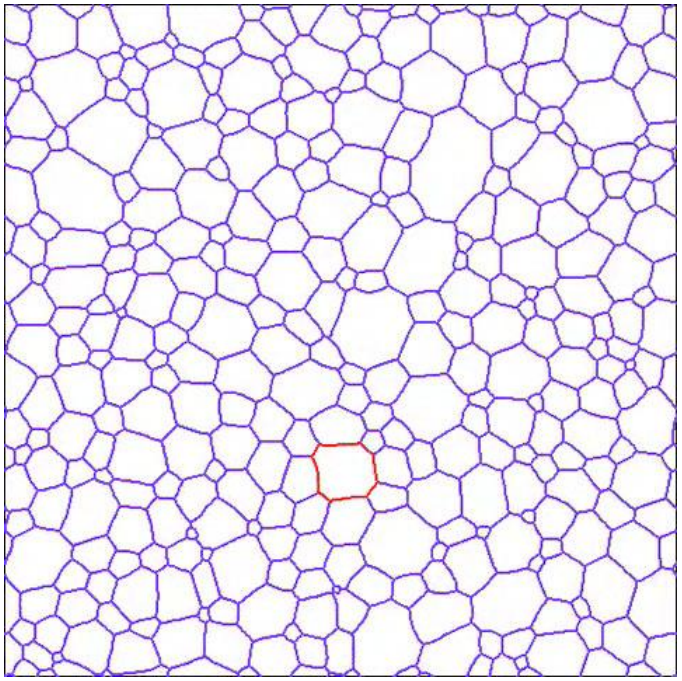

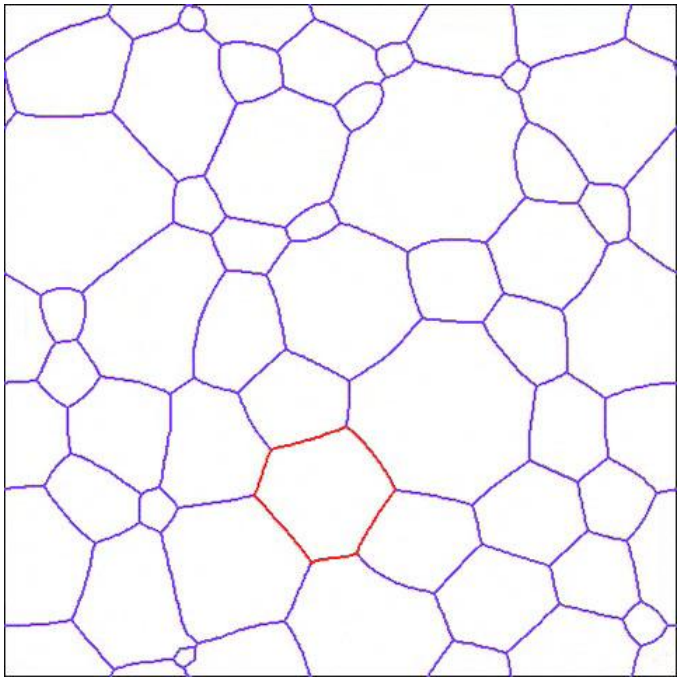

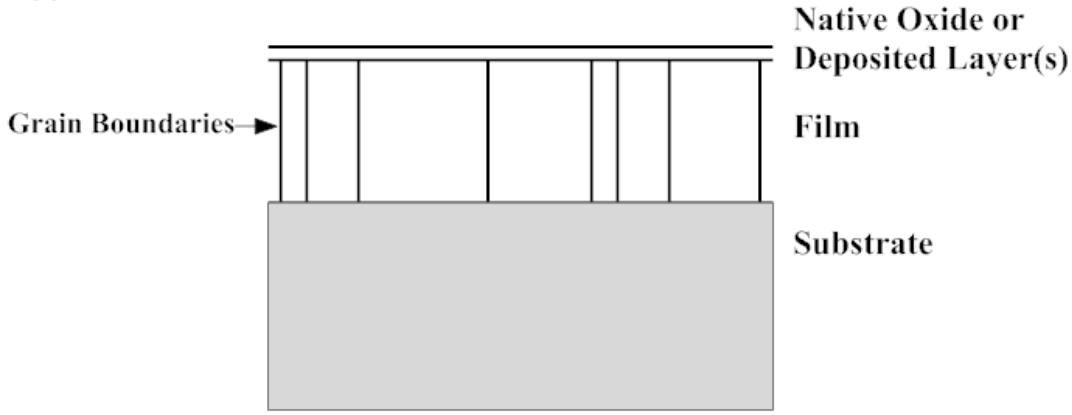

Definitions, Equilibrium at Triple Junctions and Boundary Motion

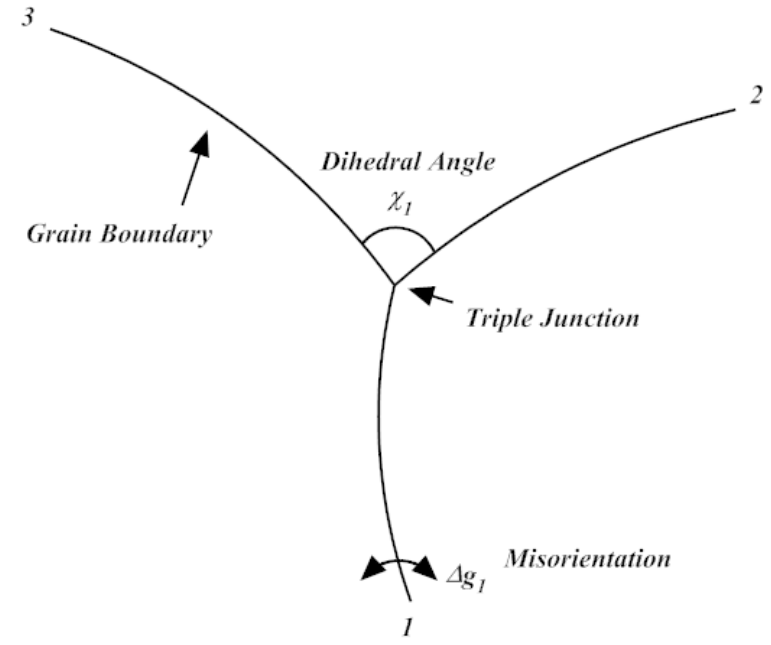

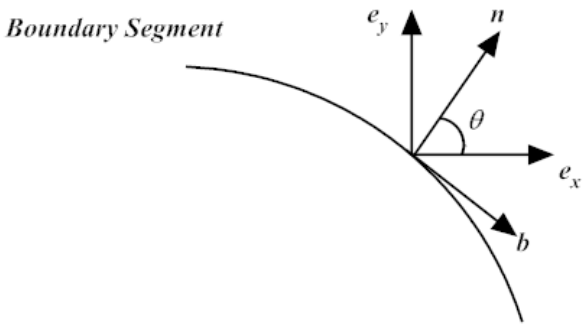

- Grain boundaries are smooth curves that meet at triple junctions or at the outside border of the configuration
- Boundary motion is curvature driven

$$\frac{d}{dt}E(t) = \sum_{k=1}^{K} \int_0^1 T^k \cdot \frac{dv^k}{ds} ds$$

$$T^k = \frac{\partial \sigma^k}{\partial \theta} n^k + \sigma^k b^k$$

Capillarity stress vector

Definitions, Equilibrium at Triple Junctions and Boundary Motion

- The Herring condition of normal and tangential force balance is enforced at triple junctions
- Maximum rate of boundary energy reduction in the interval between critical events occurs when boundaries move in the direction of their normals

$$\frac{d}{dt}E(t) = -\sum_{k=1}^{K}\int_{0}^{1}\frac{1}{\mu^k}\left|v_n^k\right|^2 ds \le 0$$

C. Herring, The Physics of Powder Metallurgy. ed. W. E. Kingston, (McGraw-Hill Book Co., New York1 951) p. 143.

$$v_n^k = \mu^k\left(\frac{d^2\sigma^k}{d\theta^2} + \sigma^k\right)\kappa^k$$

In the absence of torque terms $v_n^k = \mu^k\sigma^k\kappa^k$

Grain Growth Simulations

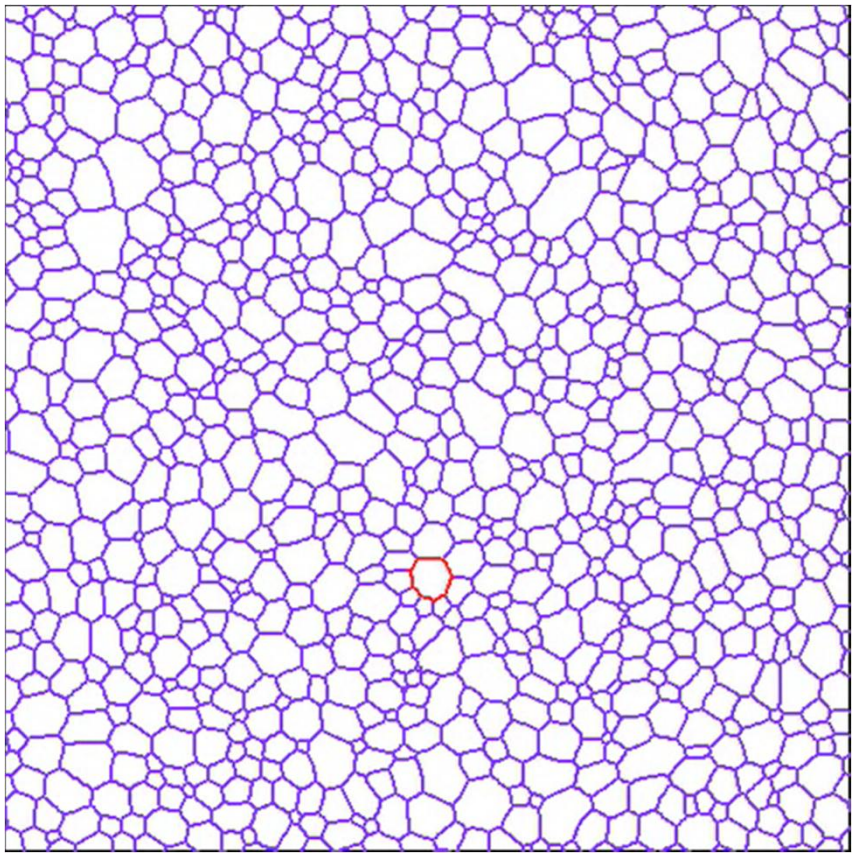

Simulation Results: Normal Grain Growth

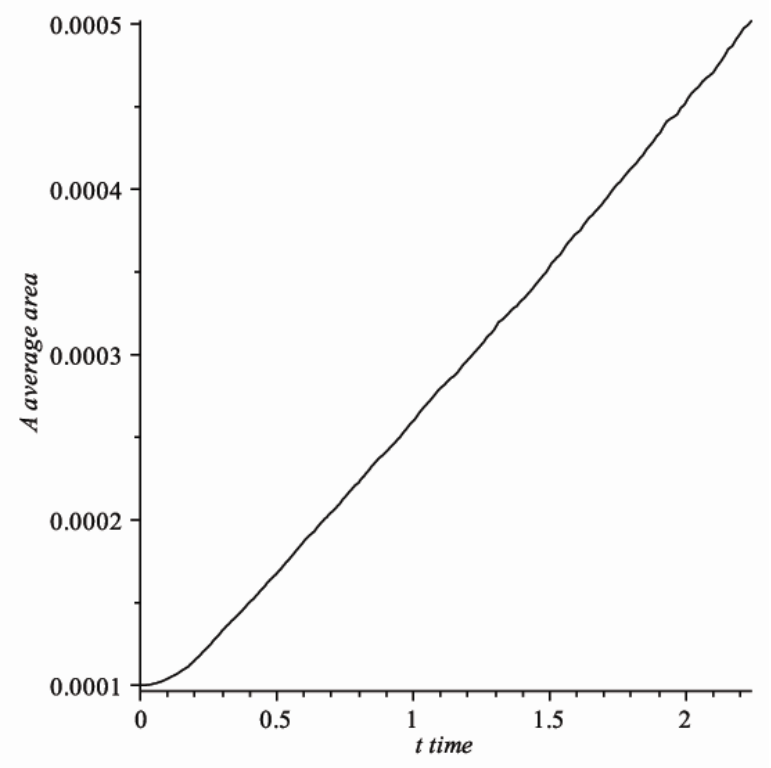

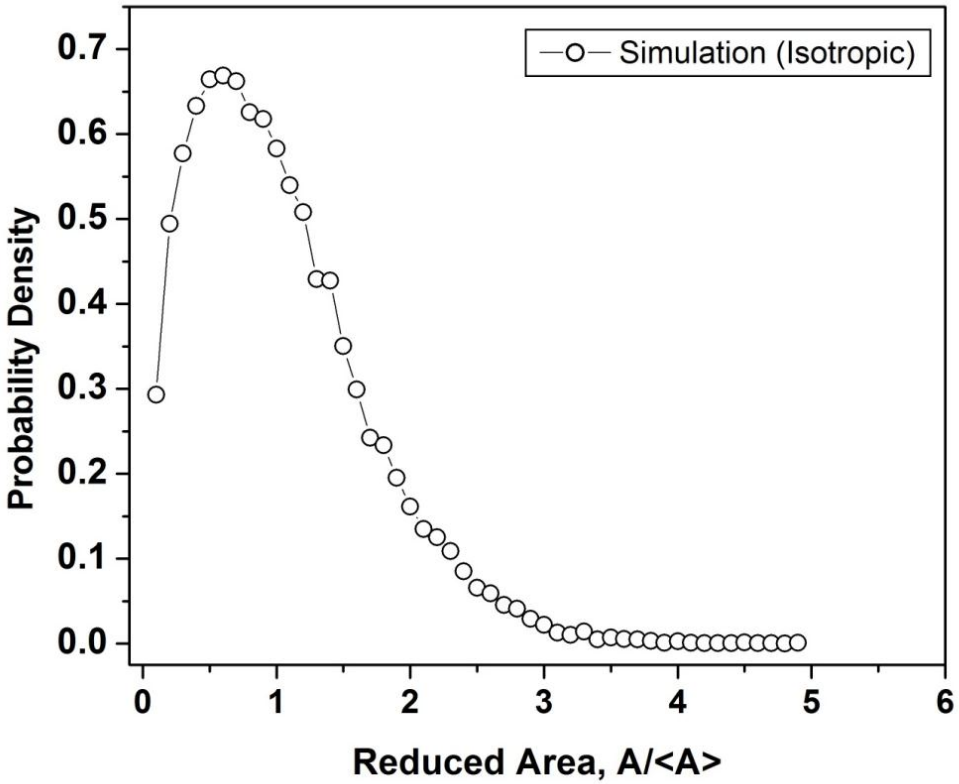

Isotropic boundary energy: Von-Neuman Mullins (n-6) rule obeyed

Von Neumann-Mullins Rule

Applies only during the period between critical events of grain disappearance and neighbor switching. Mean areas of 3, 4 and 5-sided grains are growing!

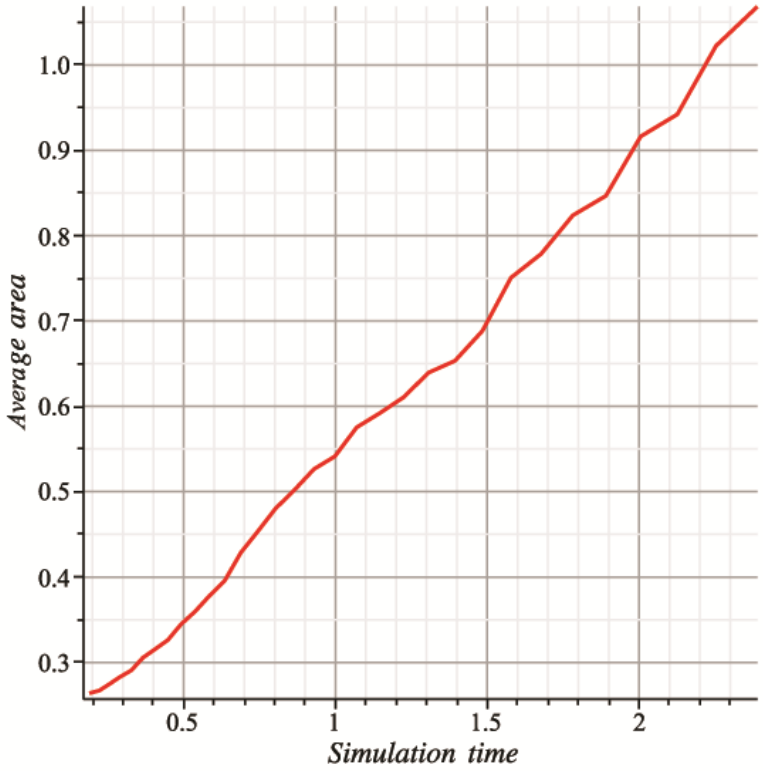

Simulation: 5-sided grains

Outline

- Introduction
- Experiments
- Simulations
- Comparison of Experiments and Simulations
- Summary and Conclusions

Metrics for Comparison of Experiments and Simulations

- Geometric
  - Size
  - Dihedral Angle Distribution
- Topological
  - Sides
  - Average Side Class of Neighbors
- Geometrical-Topological
  - Size-Sides

Experiment vs. Simulation

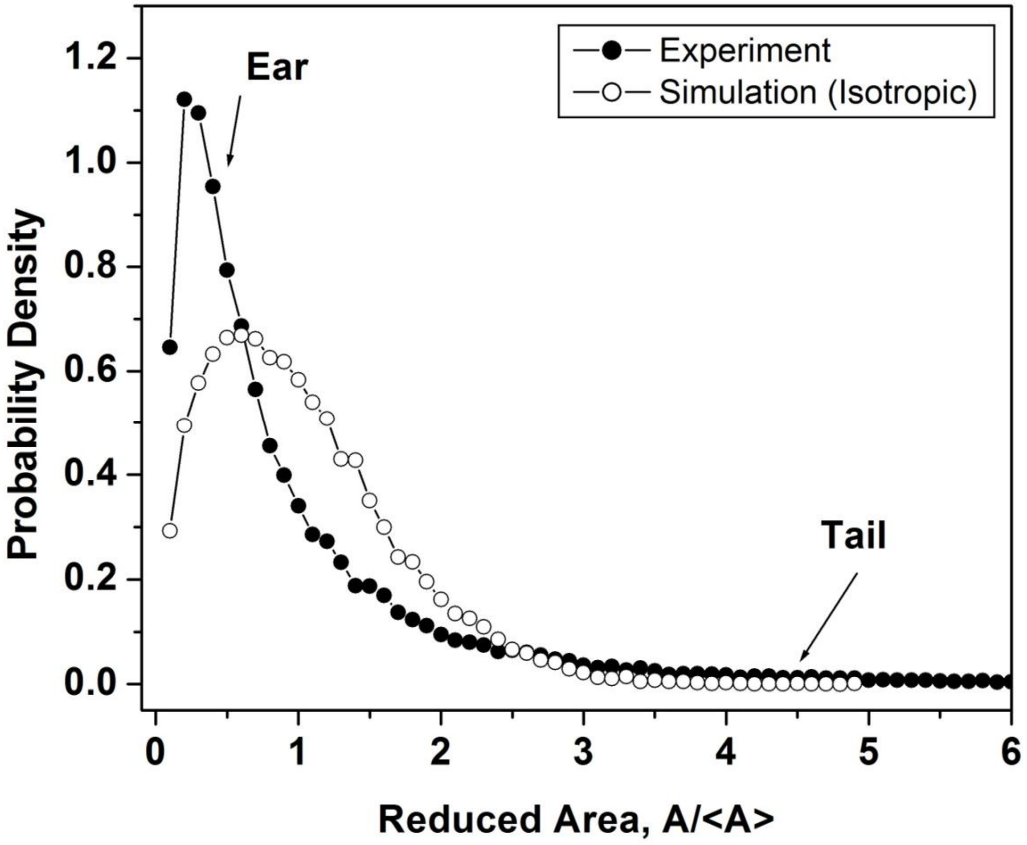

Geometry

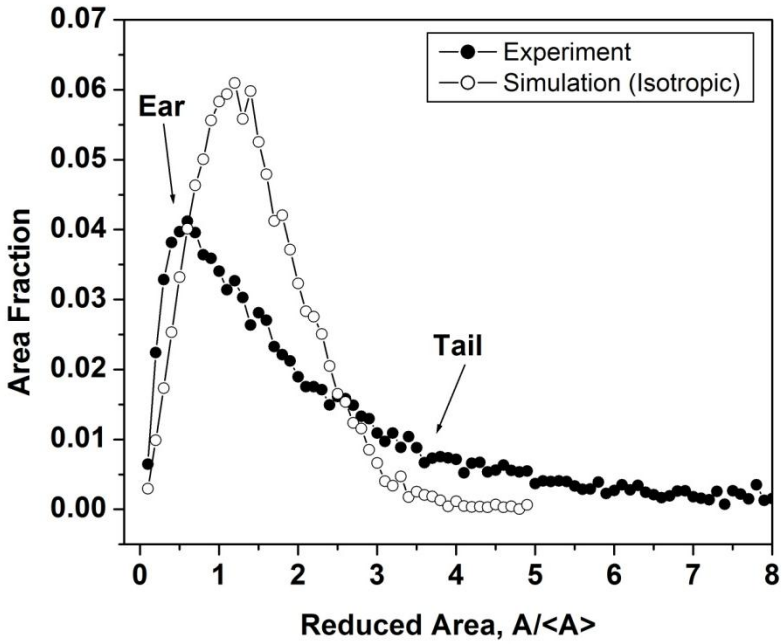

Experiment vs. Simulation

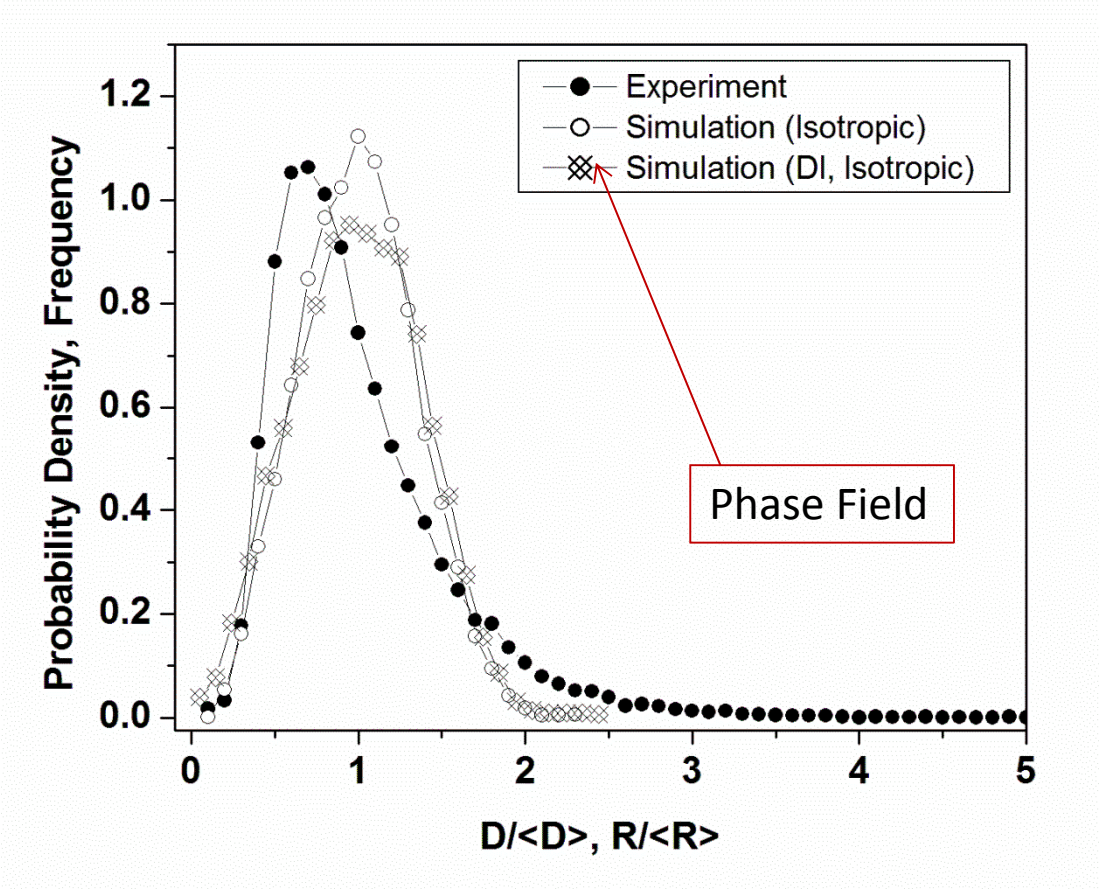

Phase Field and PDE agree reasonably well

*Kim et al., PRB **74**, 061605 (2006)*

Experiment vs. Simulation

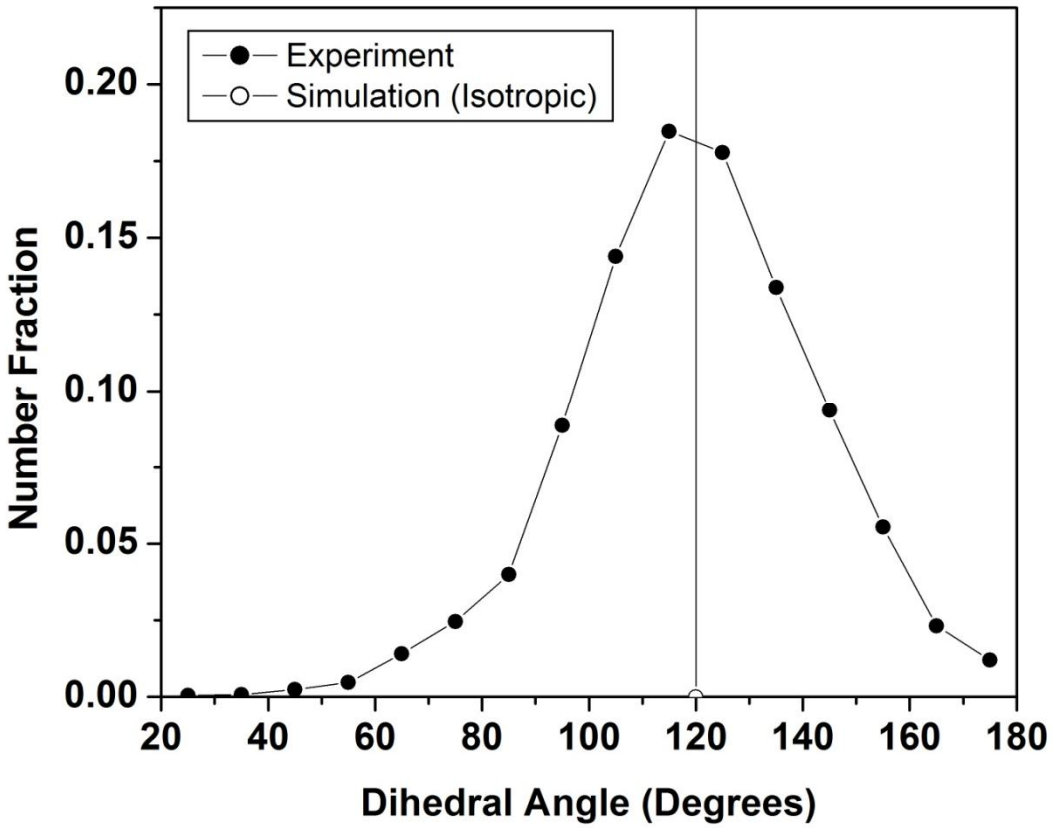

Geometry

Clear disagreement between experiment and simulation.

Experiment vs. Simulation

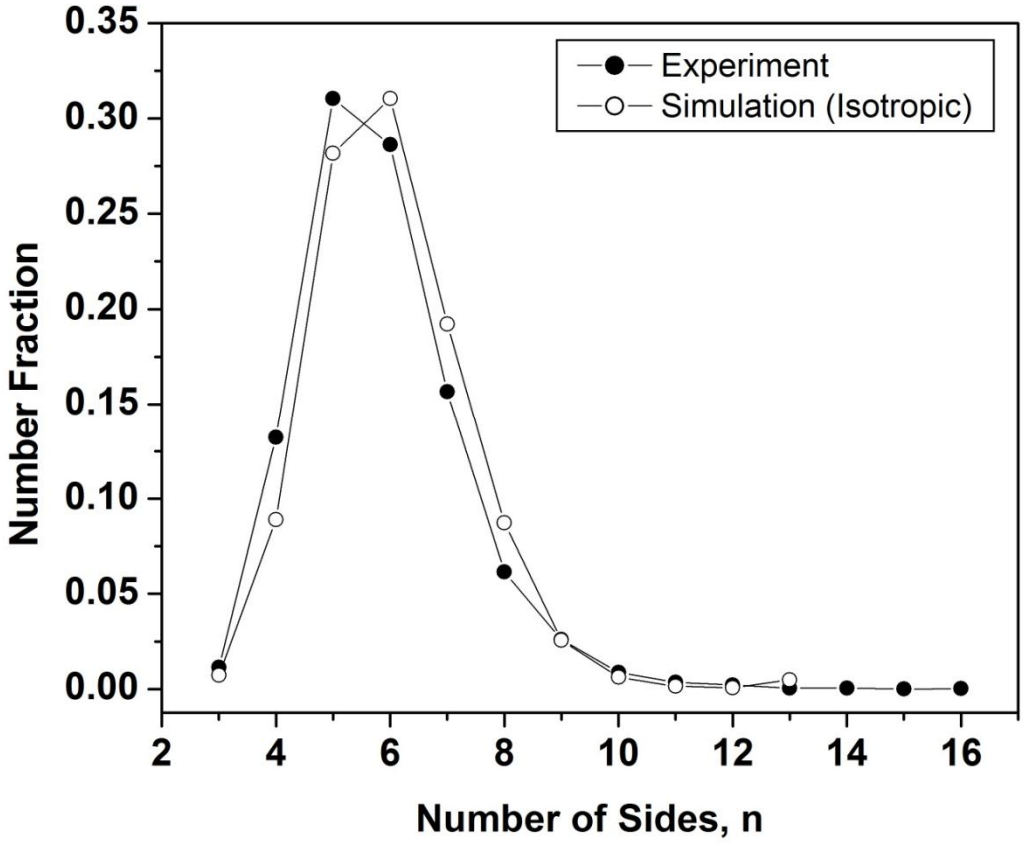

Topology

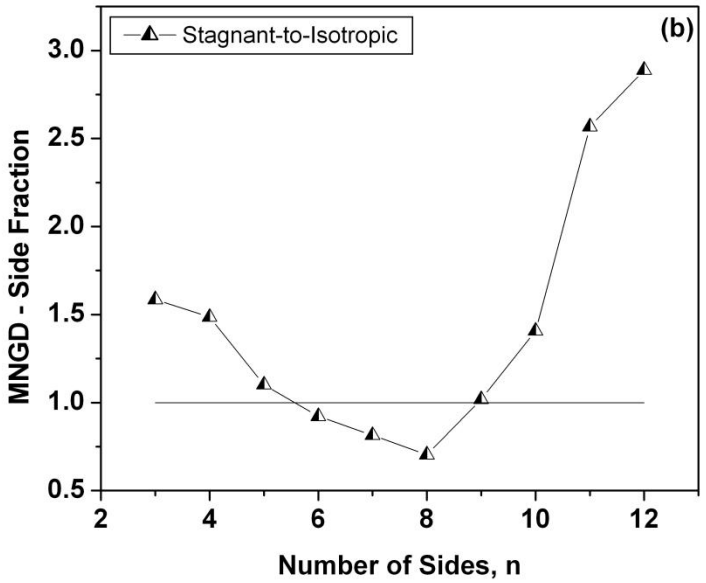

Small, but significant difference?

Experiment vs. Simulation

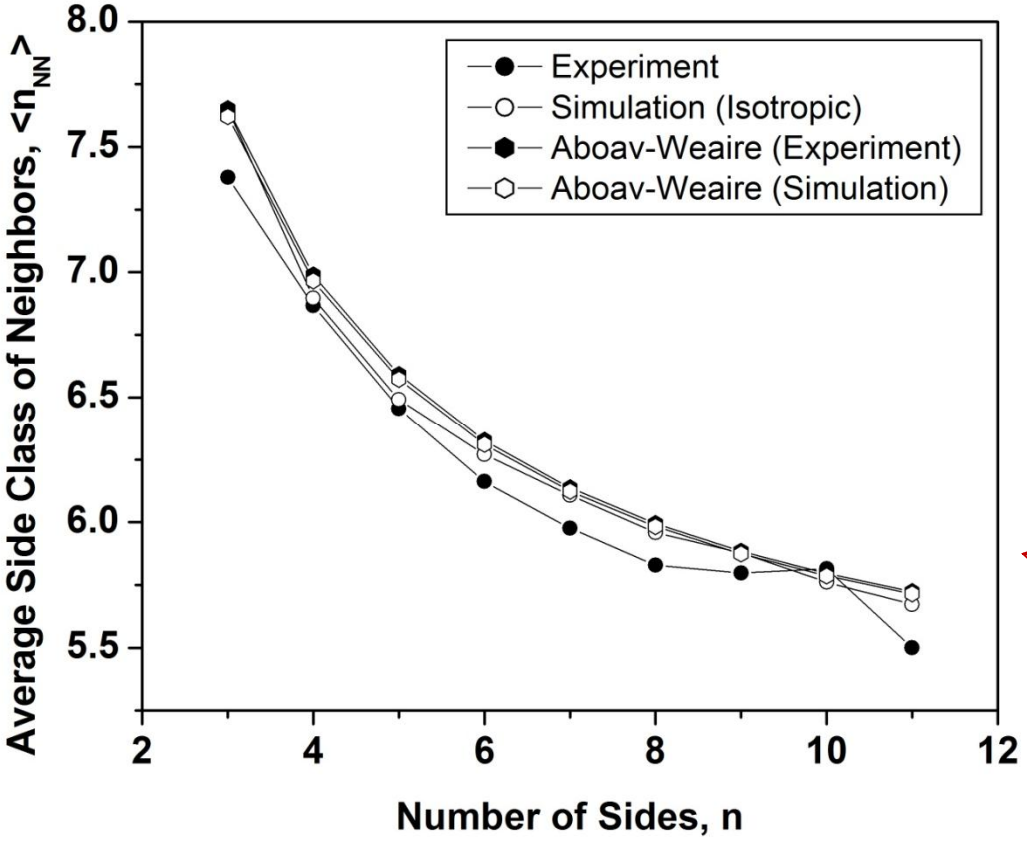

Topology

$$< n_{NN} >= 5 + \left(\frac{6 + \mu_2}{n} \right)$$

$$\mu_2 = \sum_{n=1}^{\infty} (n-6)^2 g(n)$$

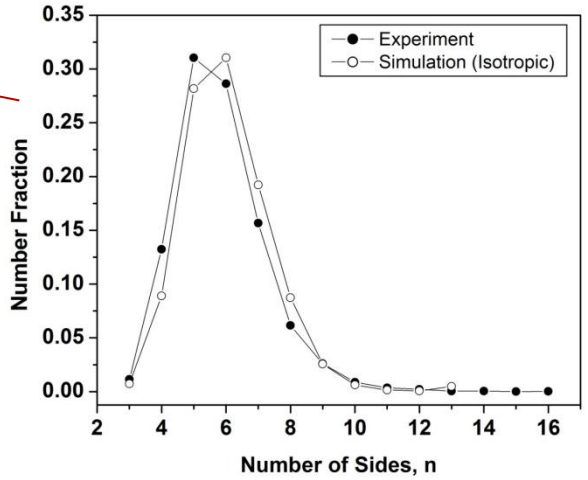

Similar trend, good agreement.

*D. Aboav, Metallography **3**, 383-390 (1970).*

Experiment vs. Simulation

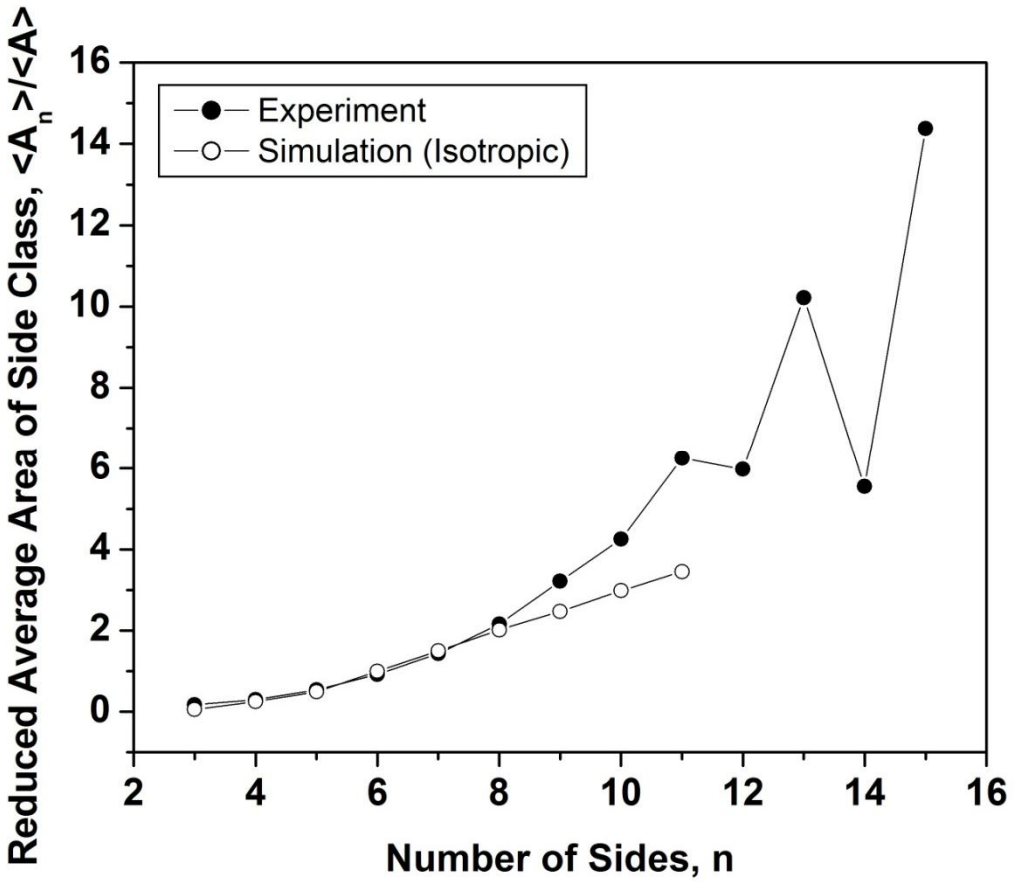

Geometry -Topology

Grains with n>8 are significantly larger in experiment than in simulation.

Experiment vs. Simulation

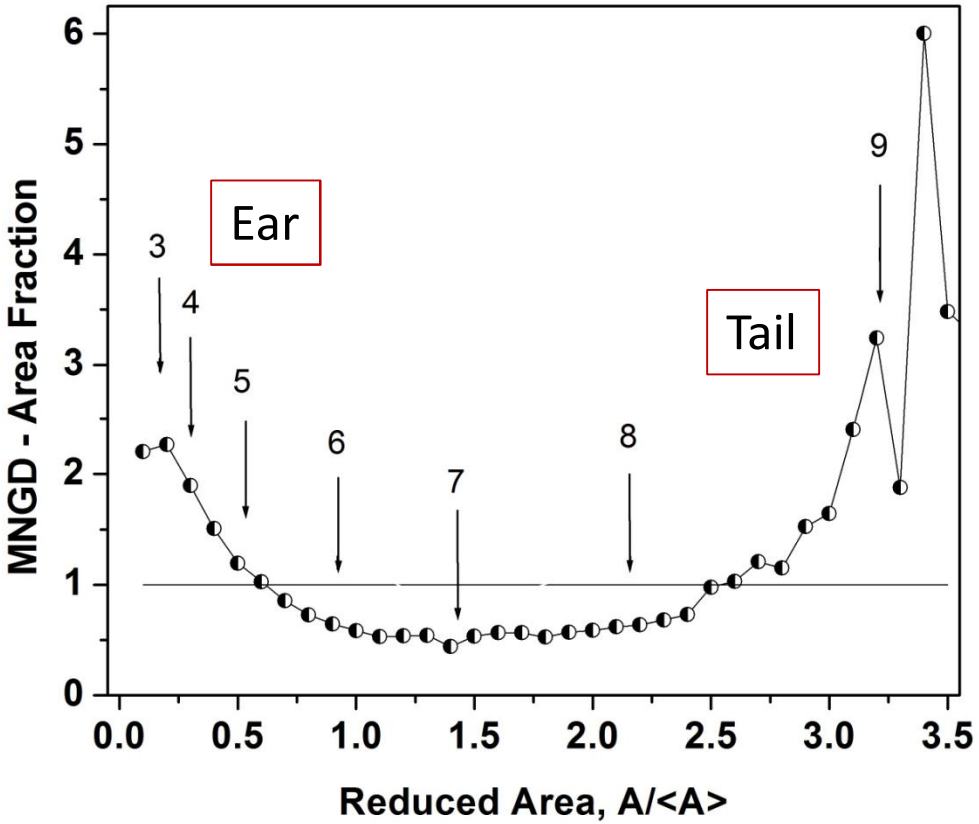

Geometry -Topology

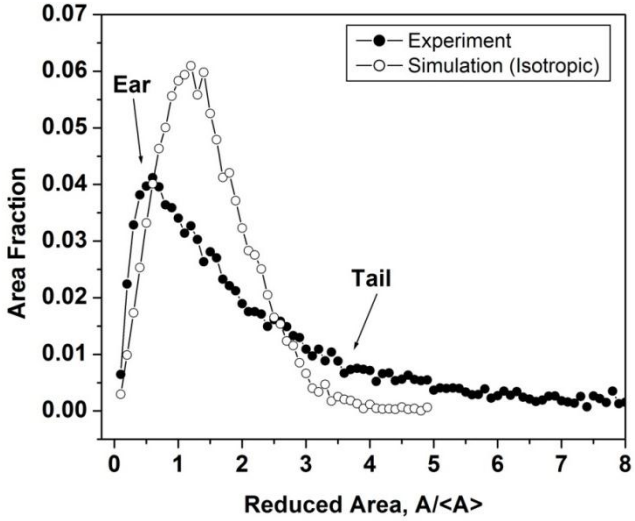

The excess of grains in the “ear” are 3 and 4 sided. The excess of large of grains are >8 sided. These excesses for large and small grains are balanced by a deficiency of 6-8 sided grains.

Five Causes to be Examined

1. Anisotropy of grain boundary energy
2. Driving forces other than grain boundary energy, specifically surface and strain energy
3. Grain boundary grooving
4. Impurity drag
5. Triple junction drag

1. Anisotropy of Grain Boundary Energy

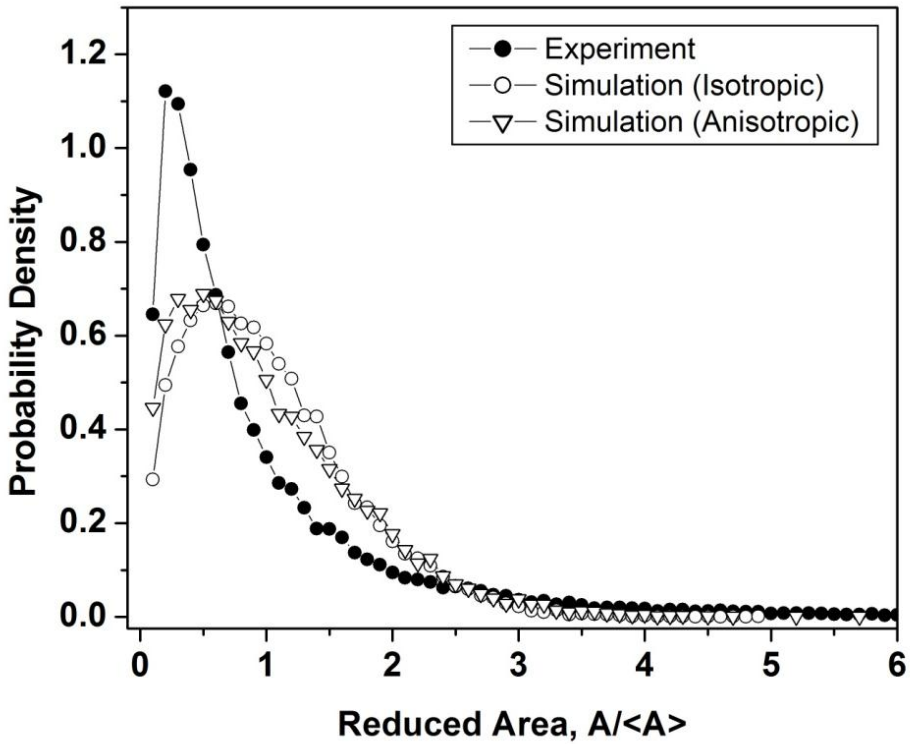

Geometry

$$\sigma = 1 + 0.125 \sin^2 2\Delta$$

Misorientation angle

1. Anisotropy of Grain Boundary Energy

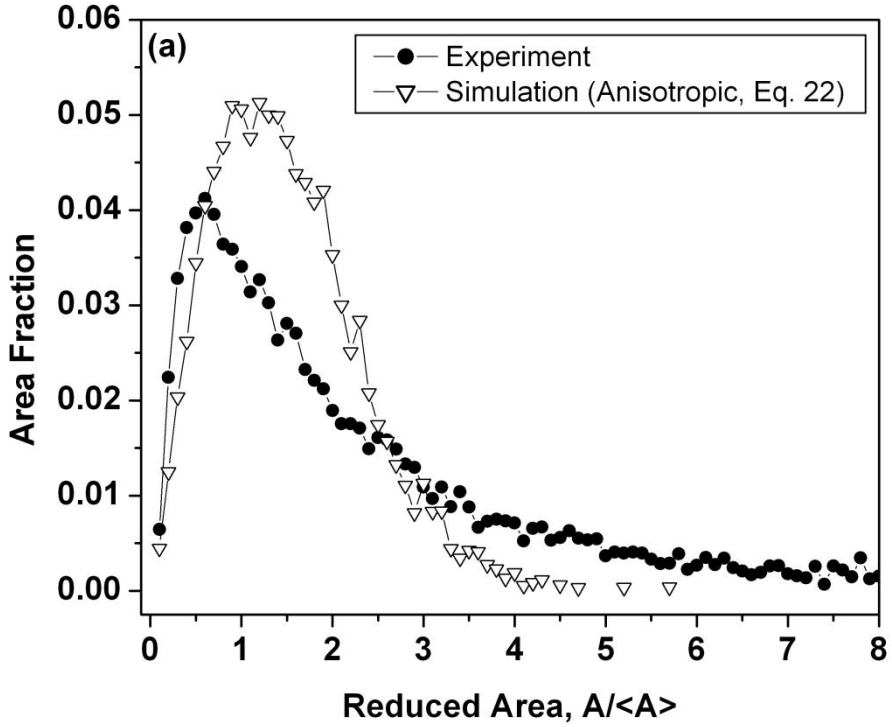

Anisotropy of grain boundary energy reduces the disagreement between simulation and experiment.

Geometry

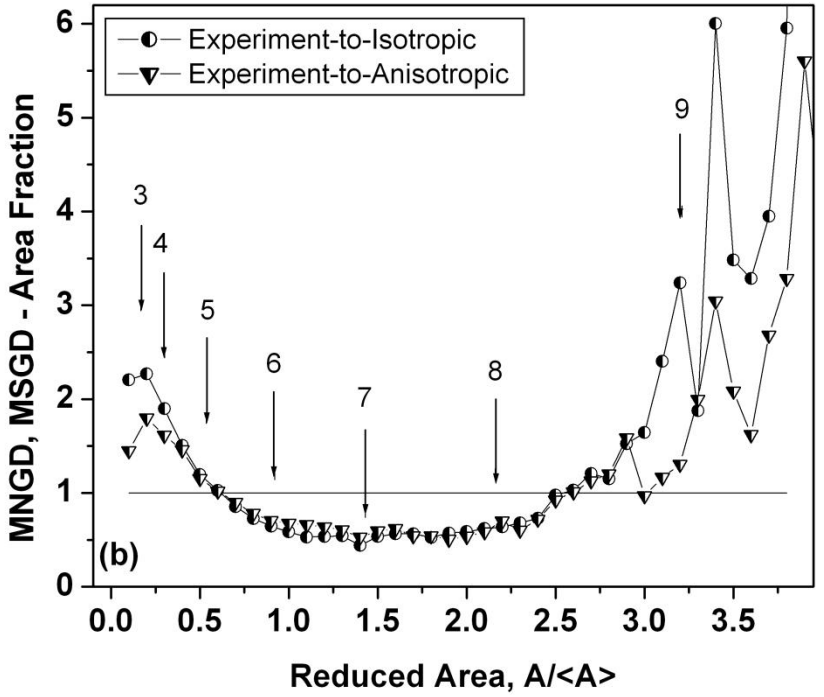

1. Anisotropy of Grain Boundary Energy

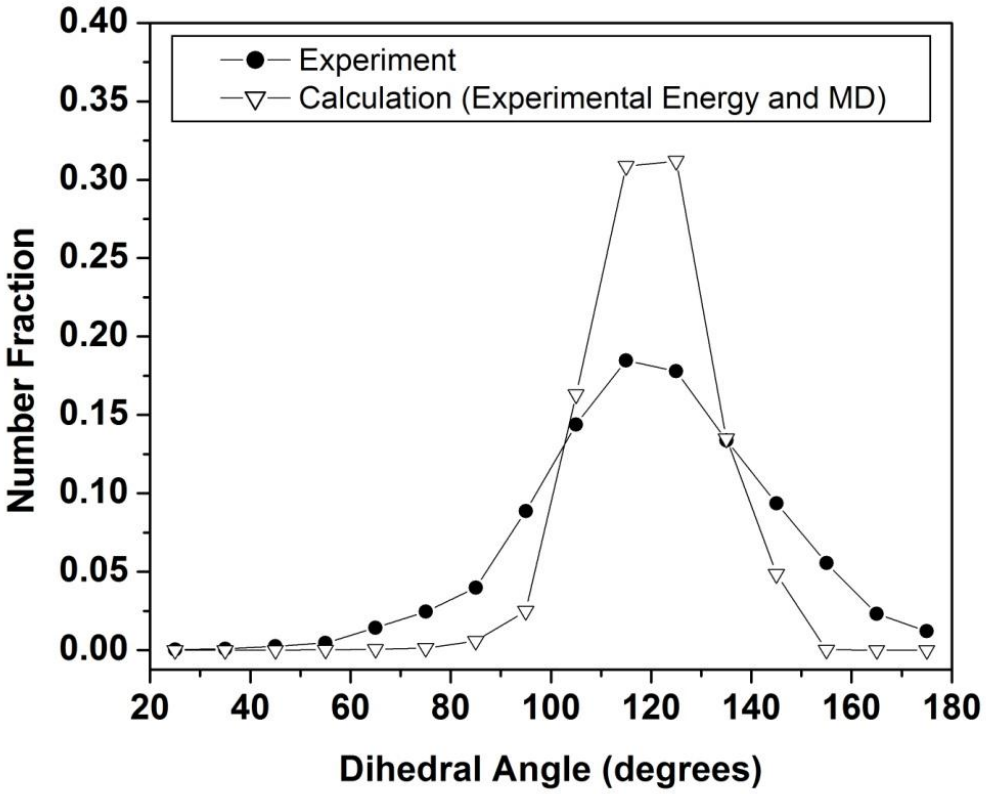

Geometry

The energy-misorientation obtained from experimental crystal orientation maps of thick Al films using a multiscale analysis method

B. L. Adams, D. E. Kinderlehrer, W. W. Mullins, A. D. Rollett, S. Ta'asan, Scripta Mater. ***38****, 531 (1998).*

Energy vs. Misorientation - Al

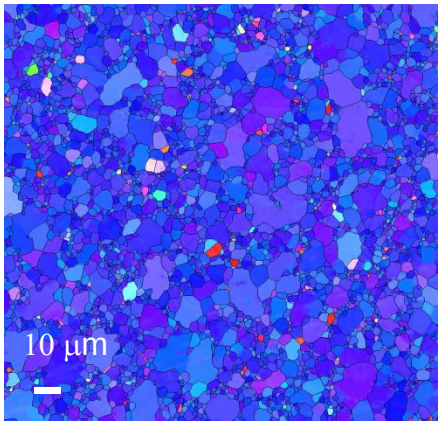

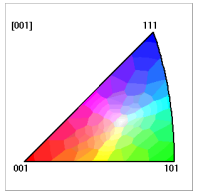

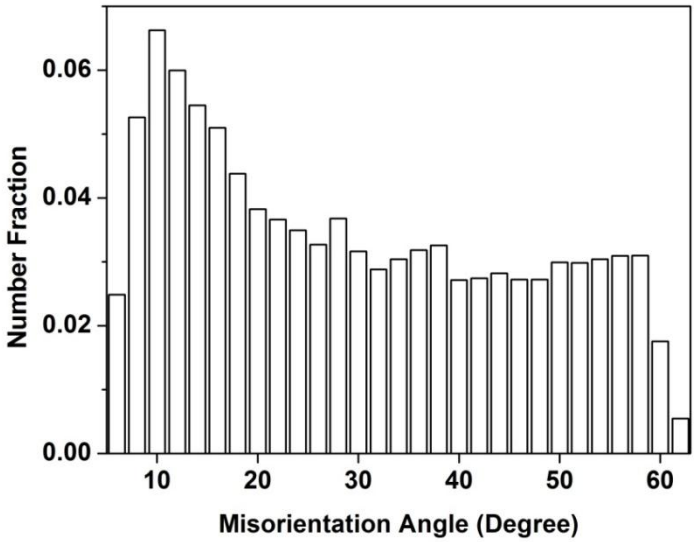

Misorientation Distribution

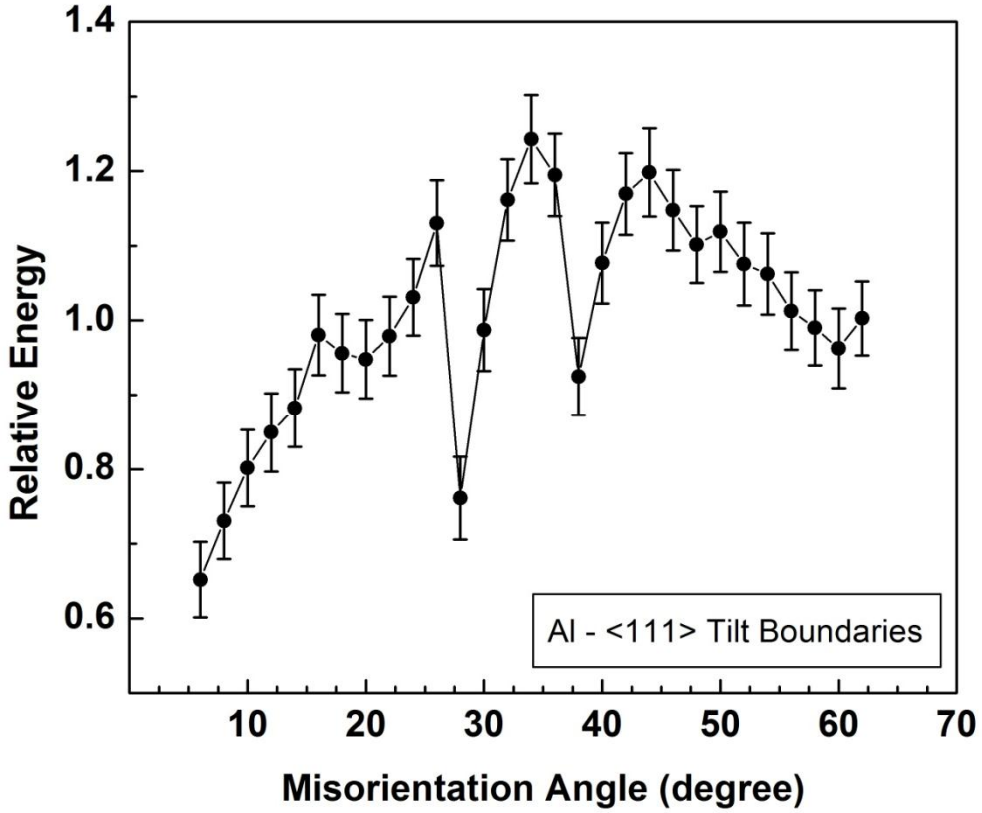

Barmak et al., Scripta Mater. ***54****, 1059 (2006).*

1. Anisotropy of Grain Boundary Energy

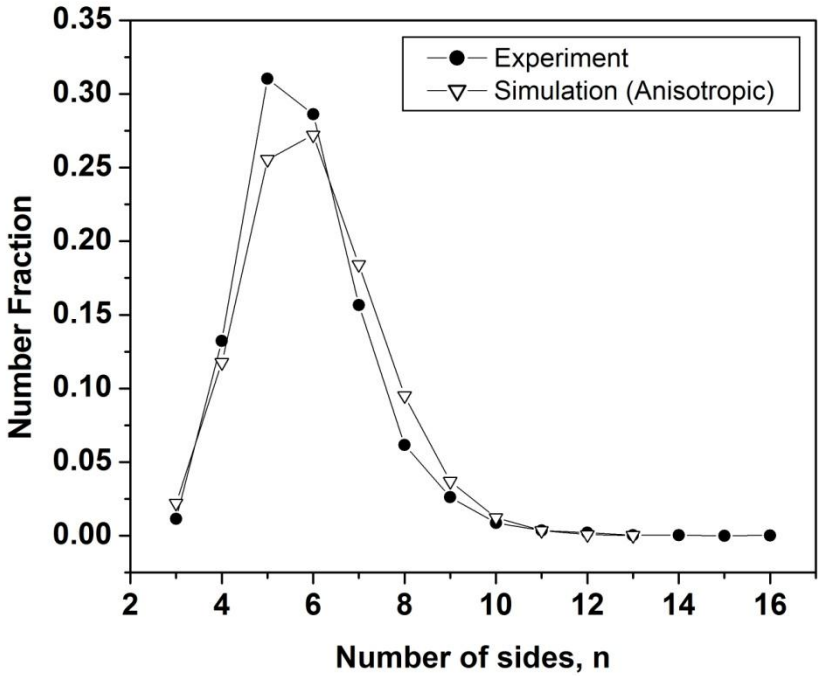

Topology

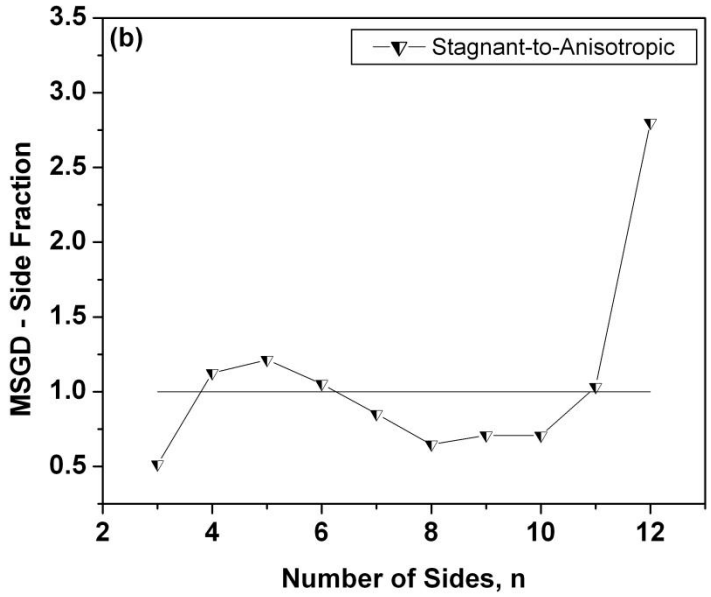

Anisotropy of grain boundary energy increases the number of 3 and 4 sided grains.

1. Anisotropy of Grain Boundary Energy

Topology

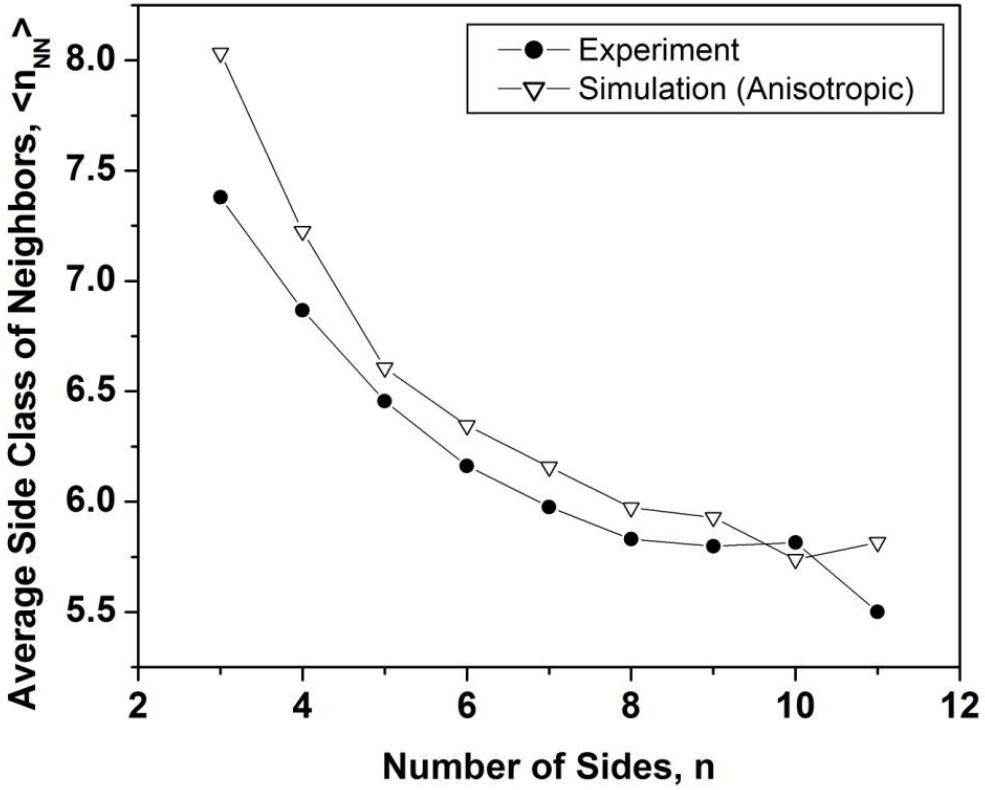

Trend remains the same and the agreement is reasonable.

1. Anisotropy of Grain Boundary Energy

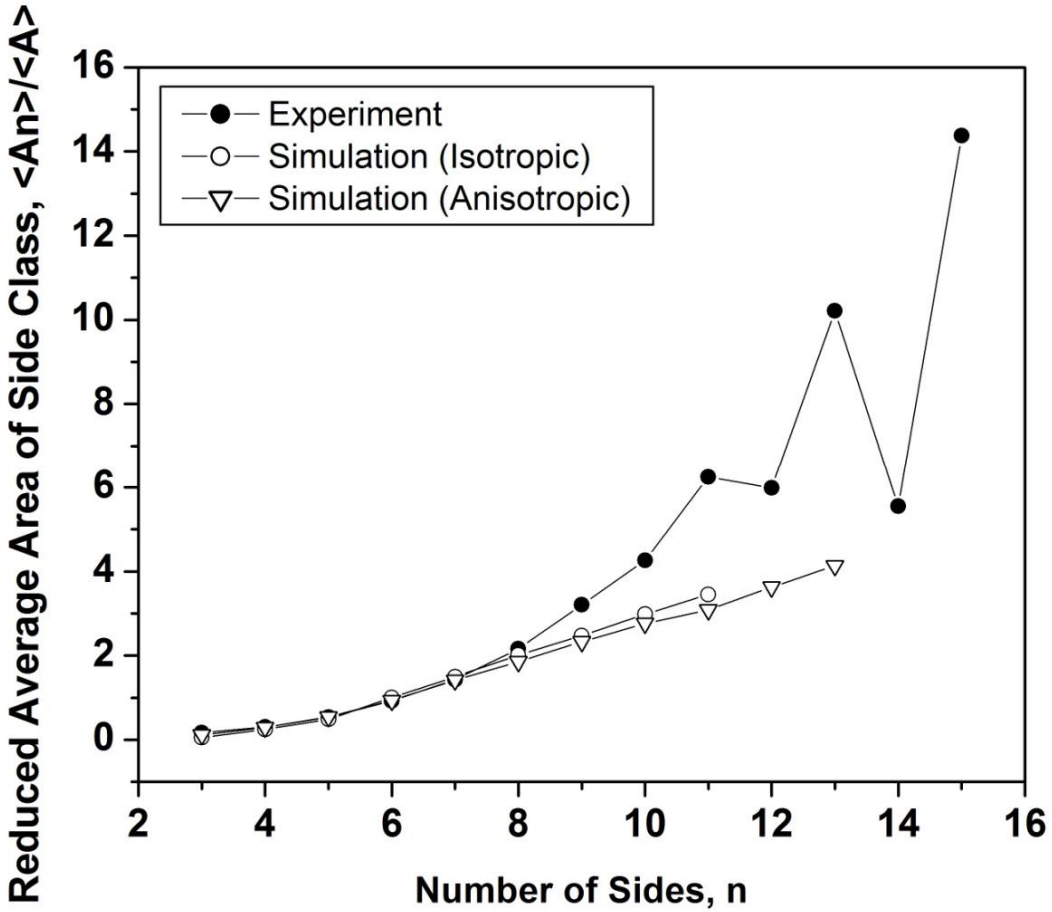

Geometry -Topology

2. Surface and Strain Energy Driving Forces

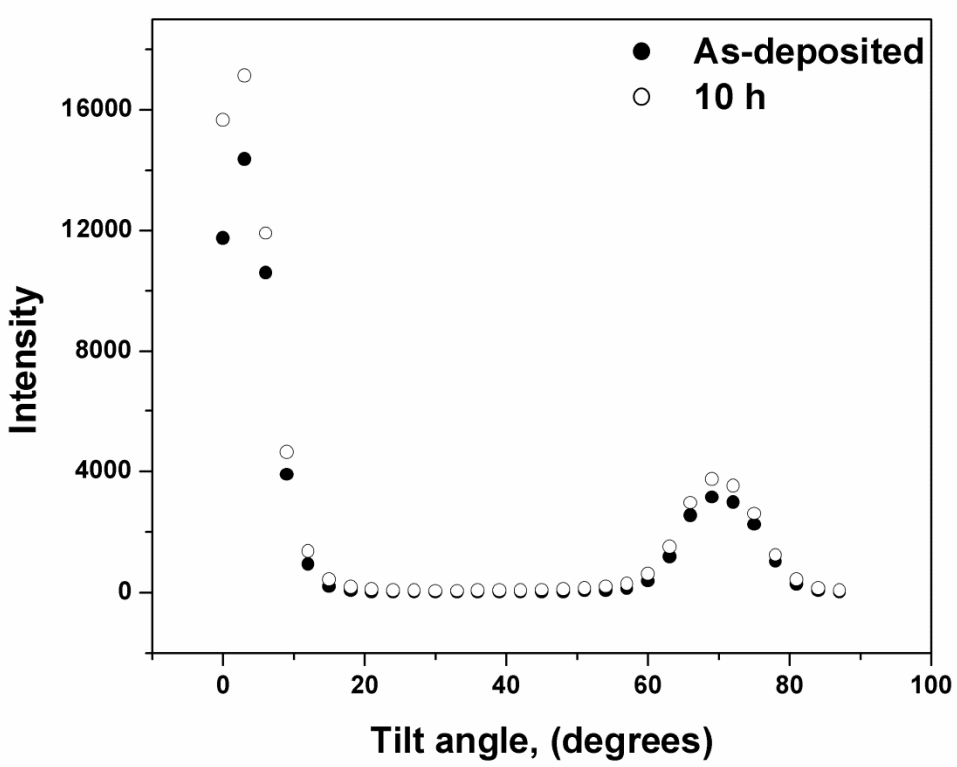

Al

111 fiber plot

Surface and strain energy anisotropy result in texture (preferred orientation) in thin films undergoing grain growth.

The Al films are strongly textured, even in the as-deposited state.
The Cu films are very weakly textured.
Yet the two sets of films exhibit the same grain size distribution.

2. Surface and Elastic Strain Energy Driving Forces

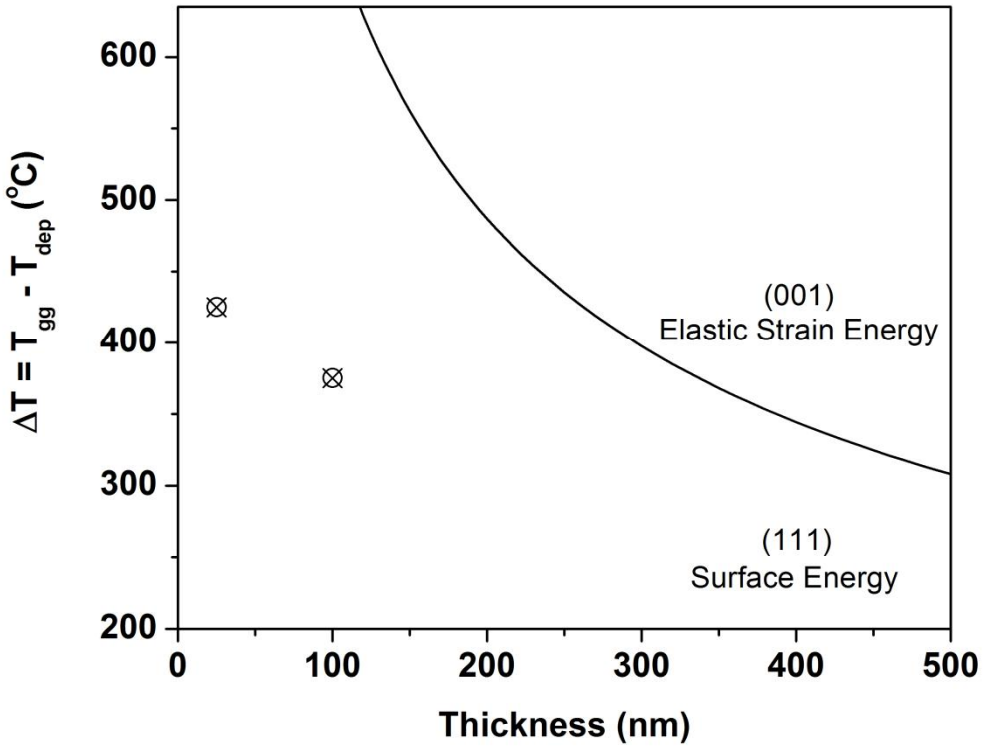

The Al films reported here are well below the thickness where elastic strain energy would affect texture evolution.

R. Carel, C. V. Thompson, H. J. Frost, Acta Metal. Mater. ***44****, 2479- (1996).*

3. Grain Boundary Grooving

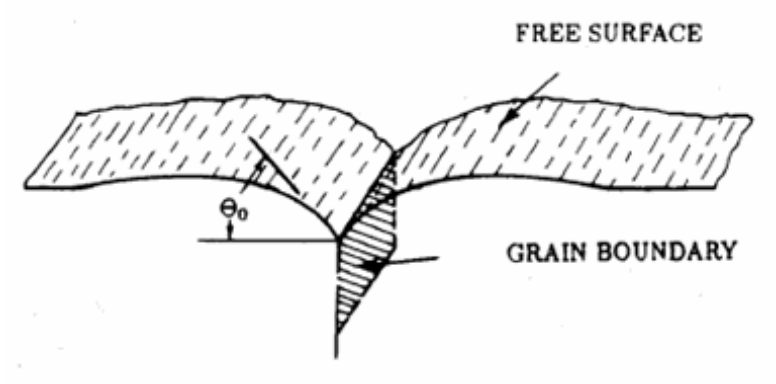

W. W. Mullins, J. Appl. Phys. ***3****, 333 (1957).*

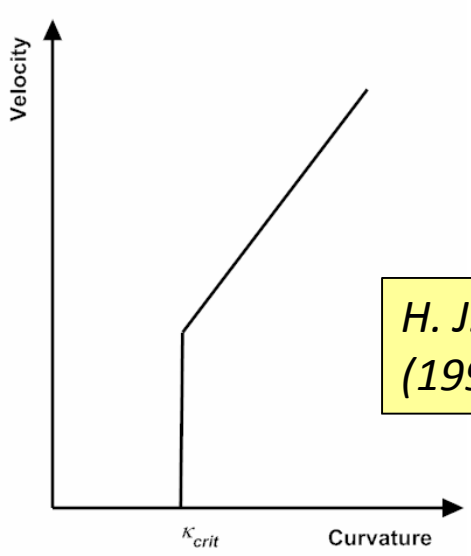

H. J. Frost, ***32****, 257 (1994).*

$$\kappa_{crit} = \frac{2\theta_o}{h} = \frac{\gamma_{gb}}{\gamma_s h}$$

3. Grain Boundary Grooving

Size distribution is found to be lognormal, but it is narrower than the experimental distribution.

Topology

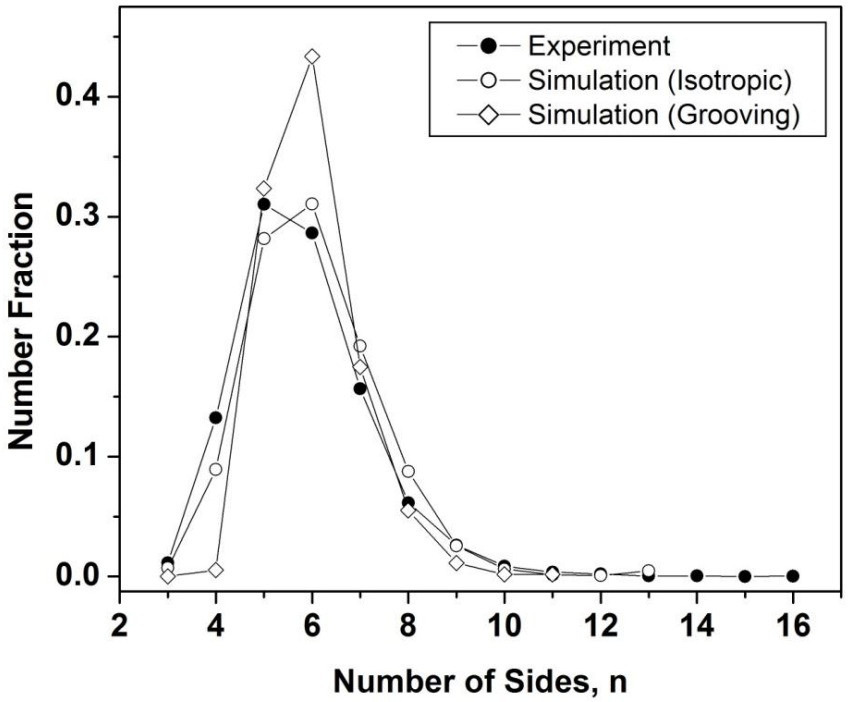

Number of 3 and 4-sided grains sharply reduced.

Agreement between experiment and simulation significantly worsened.

S. P. Riege, C. V. Thompson, H. J. Frost, Acta Mater. ***47****, 1879 (1999).*

3. Grain Boundary Grooving

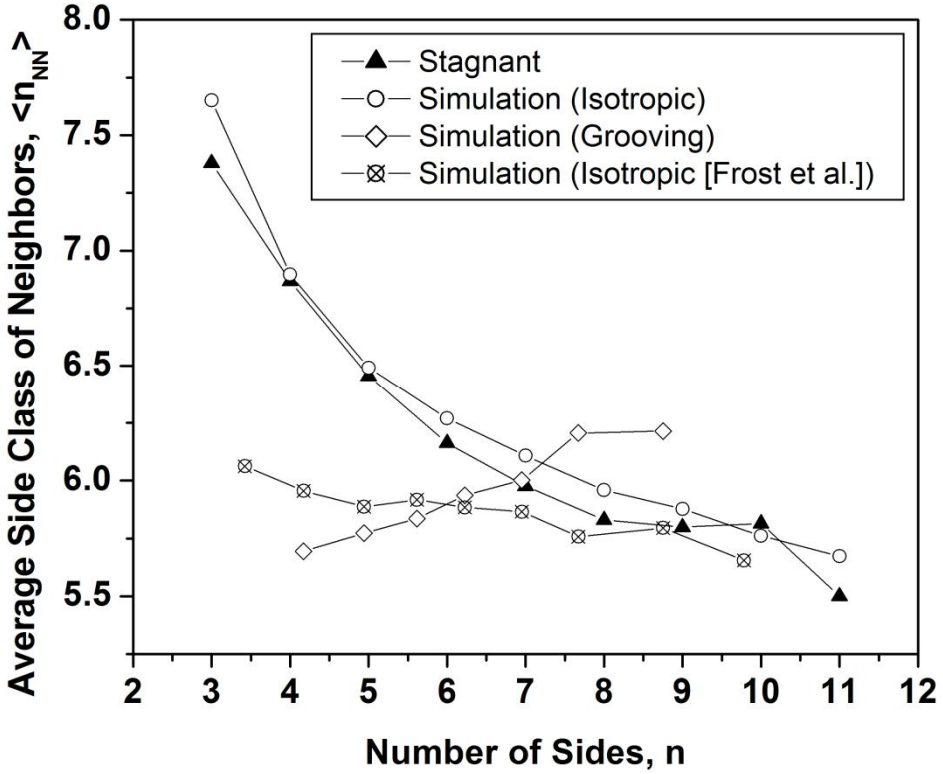

Topology

Average side class of neighbors shows the opposite trend to experiment.

H. J. Frost, C. V. Thompson and D. T. Walton, Acta Metall. Mater. ***38****, 1455-(1990).*

4. Impurity Drag

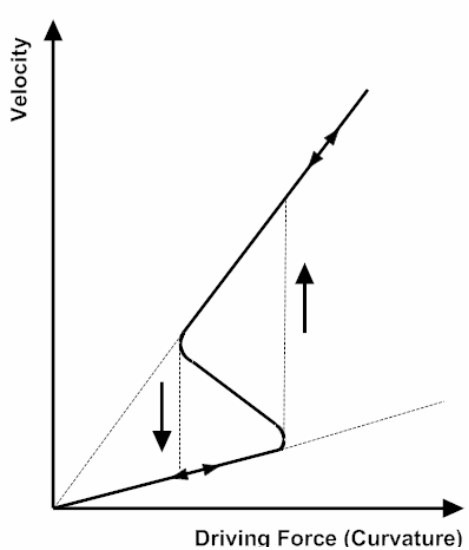

Sharp Interface Simulations – Lognormal size distribution seen for intermediate to high drag levels, as in grain boundary grooving.

Sides distribution unlikely to agree with simulation.

H. J. Frost, Y. Hayashi, C.V. Thompson and D. T. Walton, Mat. Res. Soc. Symp. Proc. ***317****, 431 (1994)*

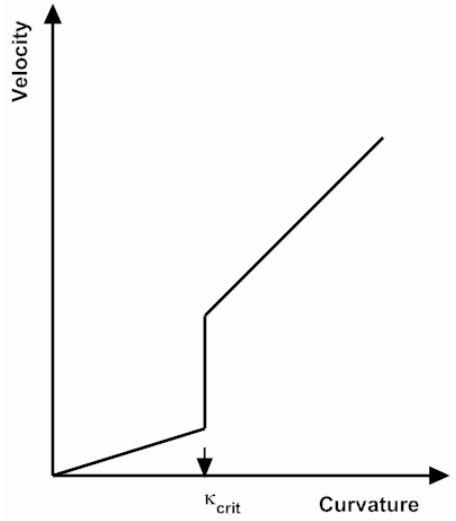

Experiment-Experiment Comparison: Calculation of impurity content (Fe) in the grain boundaries of the 100 nm-thick Al samples are found to be 10-40 times lower than that found at cessation of grain growth or saturation of boundaries in bulk Al samples.

P. Gordon and T. A. El-Bassayouni, Trans. Metall. Soc. AIME ***233****, 391 (1965).*

4. Impurity Drag

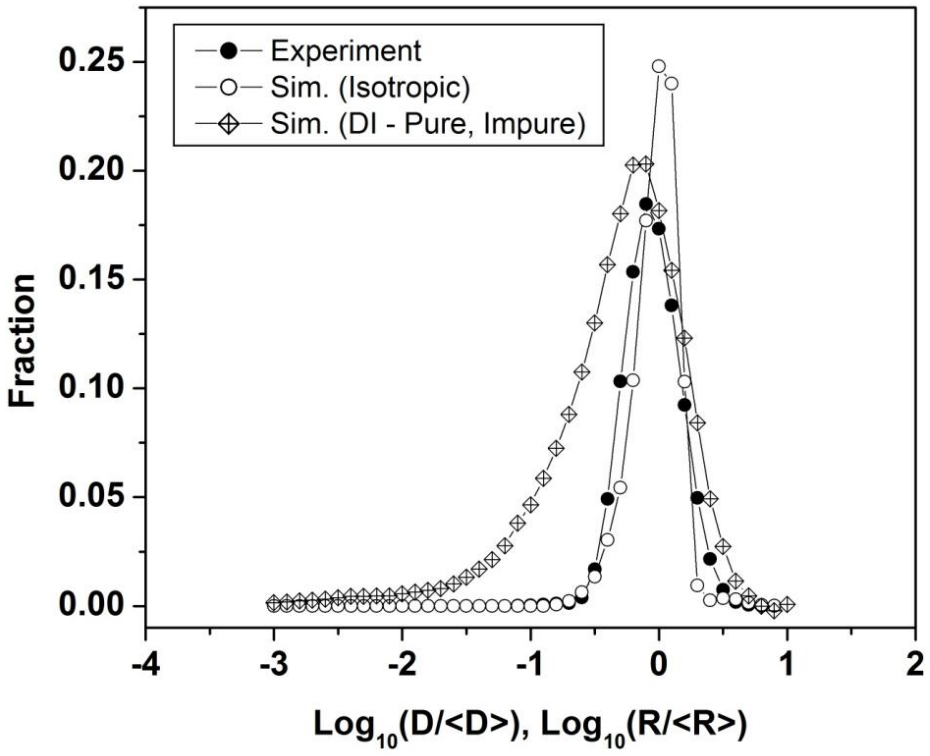

Geometry

Diffuse interface simulations – Size distribution in worse agreement than simulations with no impurity drag.
Also note the disagreement between simulations.

D. Fan, S. P. Chen, L.-Q. Chen, J. Mater. Res. ***14****, 1113 (1999).*

4. Impurity Drag

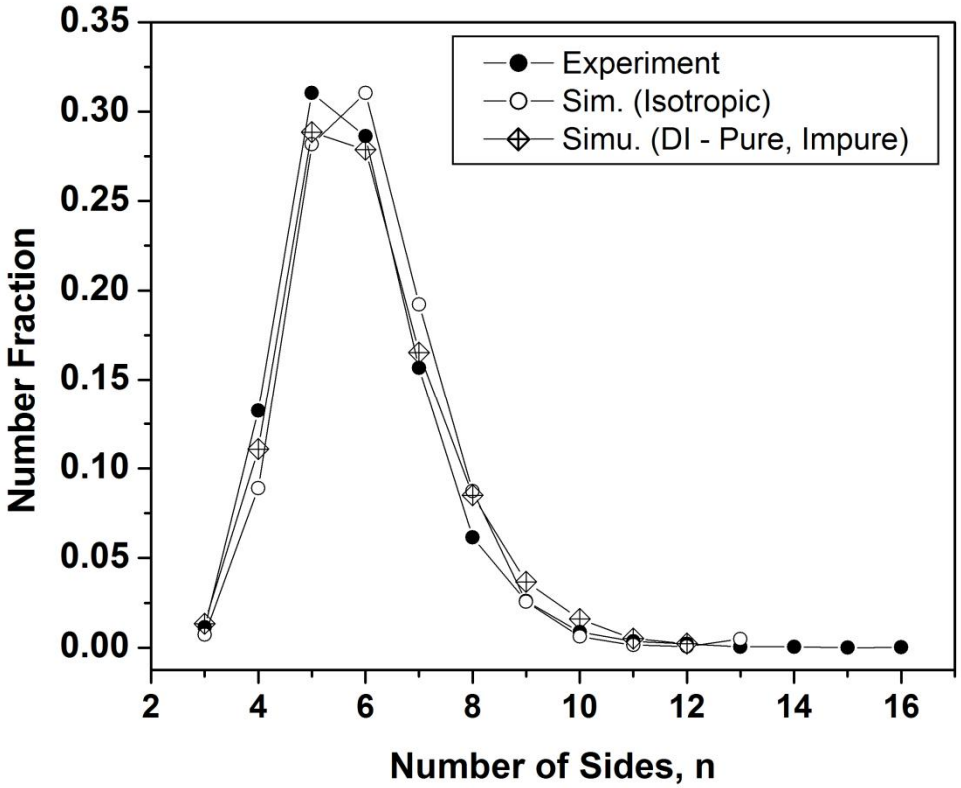

Topology

Sides distribution somewhat better agreement.

D. Fan, S. P. Chen, L.-Q. Chen, J. Mater. Res. ***14****, 1113 (1999).*

5. Triple Junction Drag

$$v_{TJ} = -\mu_{TJ} \sum_{l=1}^{3} T^{m,l}$$

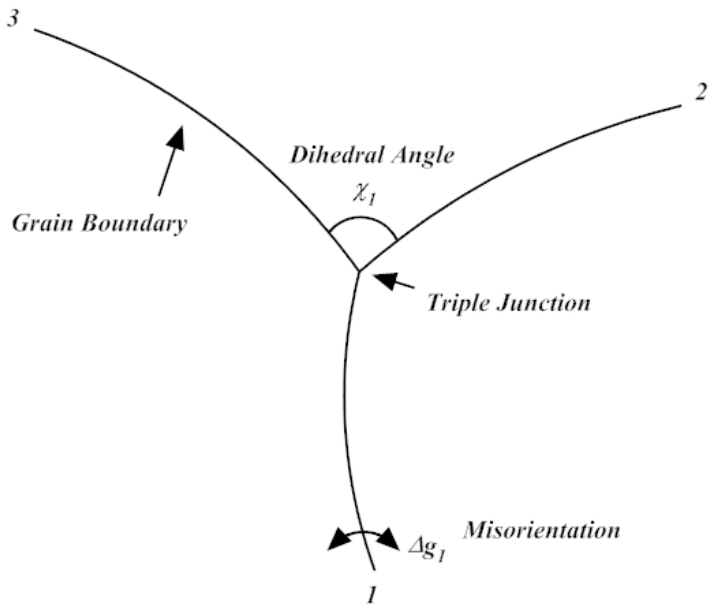

17 levels of drag examined in our simulations.

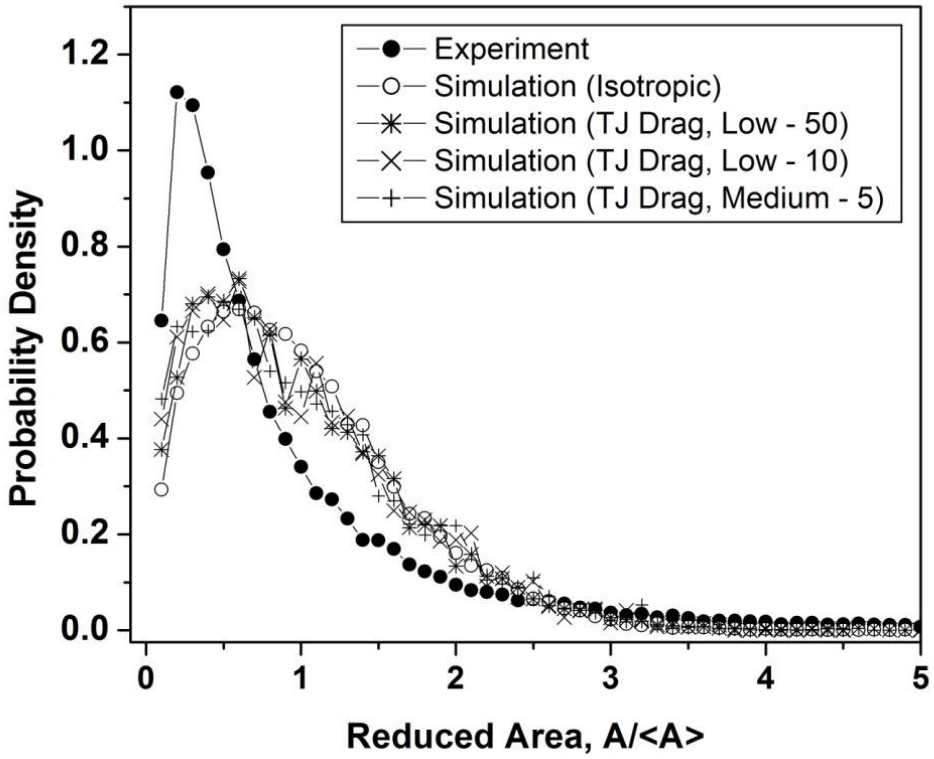

G. Gottstein and L. S. Shvindlerman, Acta Mater. ***50****, 703-713(2002).*

5. Triple Junction Drag

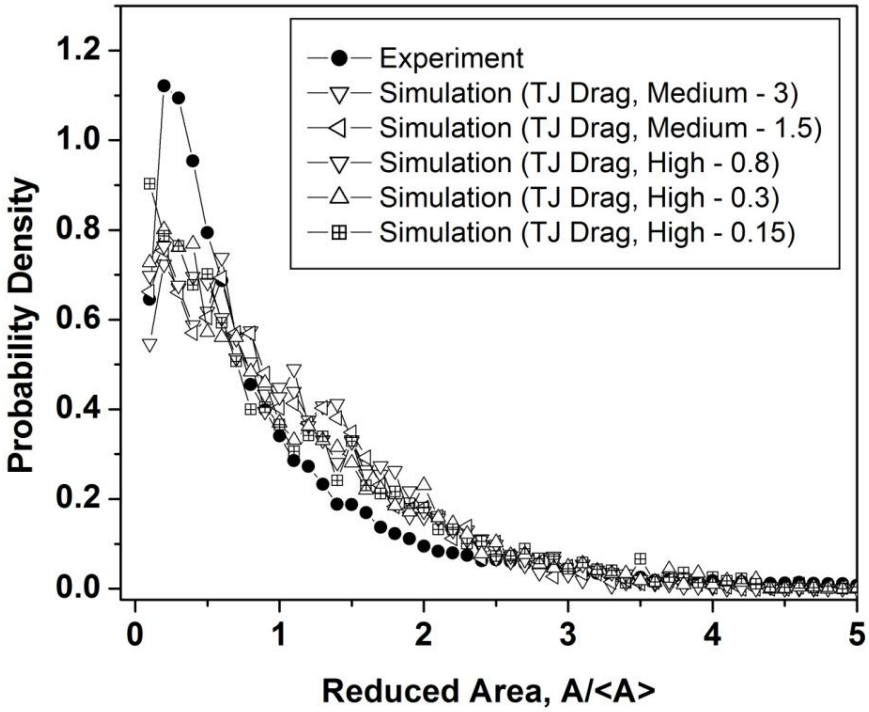

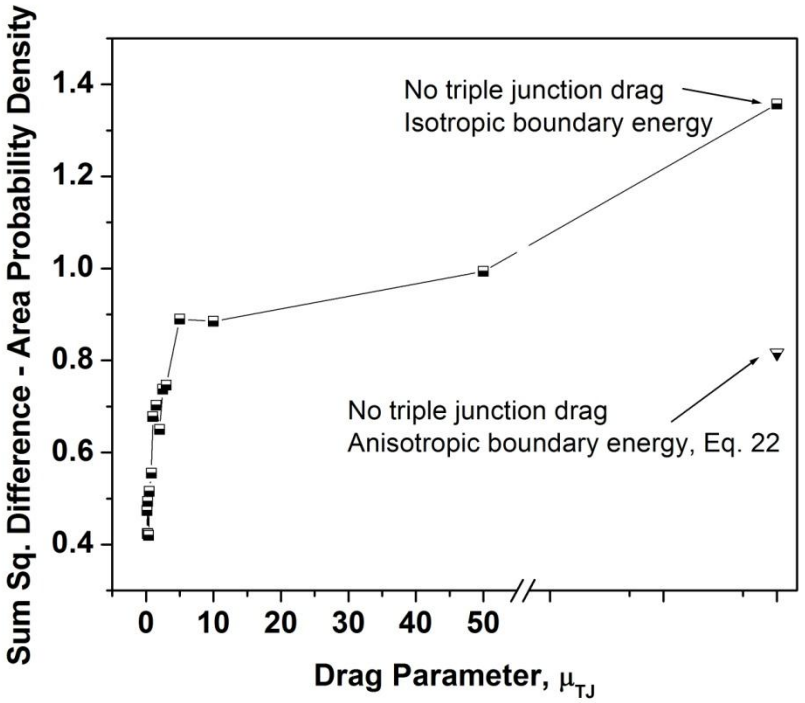

As drag parameter is decreased (drag increased), the SSD decreases, but the simulated distribution loses its peak.

5. Triple Junction Drag

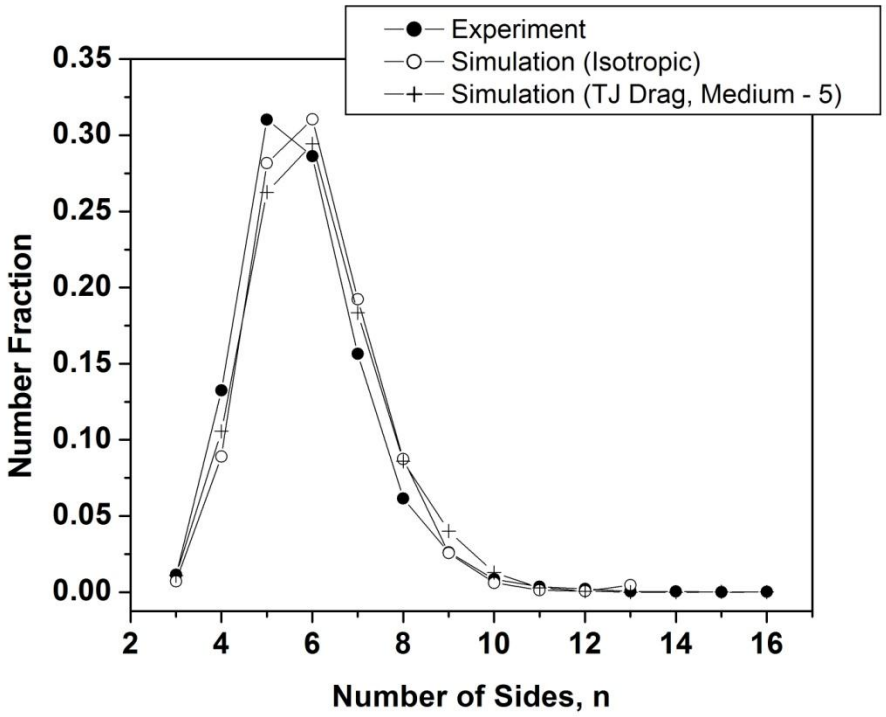

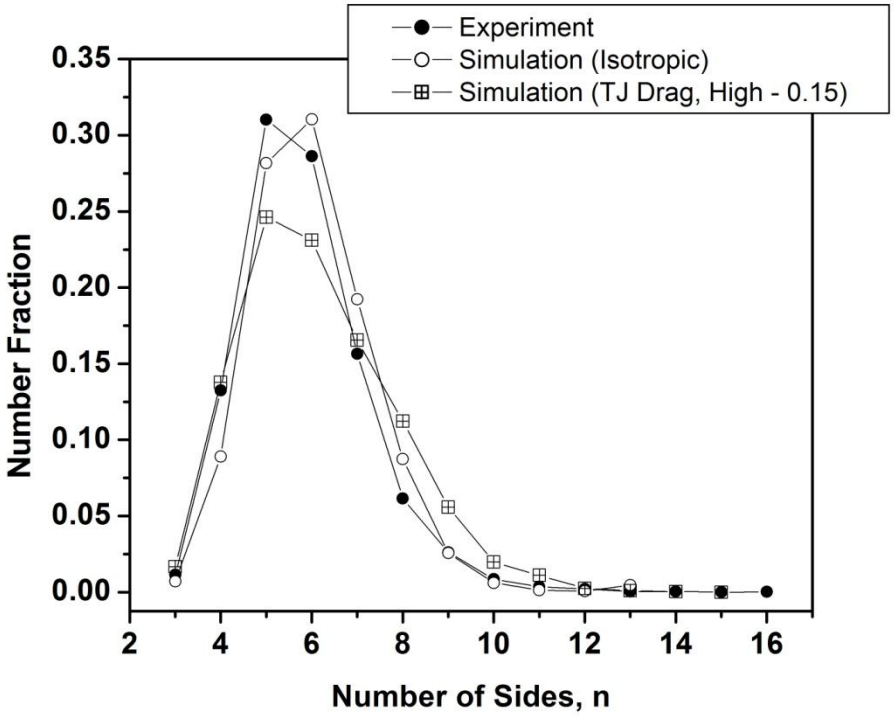

As drag parameter is decreased (TJ drag increased), the disagreement between experiment and simulation increases.

5. Triple Junction Drag

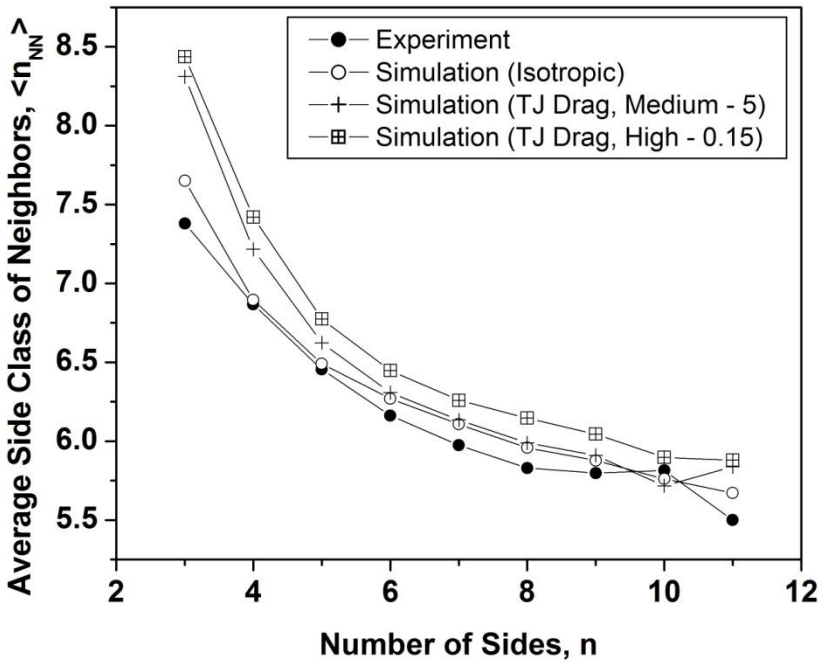

Trend not changed.

TJ drag does result in larger grains relative to the mean compared with no drag.

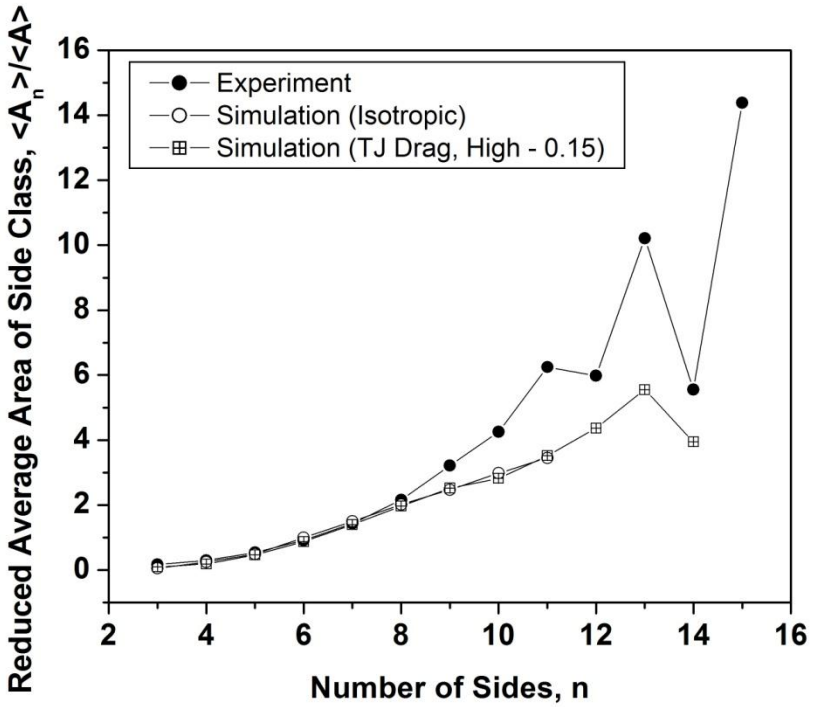

Summary and Conclusions

- The size distributions for the Al and Cu films are remarkably similar to each other despite the many and significant differences in experimental conditions, which include sputtering target purity, substrate type, film thickness, deposition temperature, actual as well as homologous annealing temperatures, annealing time, absolute grain size, and the twin density within the grains. This similarity argues for a universal experimental grain size distribution, which for grain diameters is lognormal, as found previously for thin films at stagnation.

- Comparison of the experimental grain size distribution with that for two dimensional grain growth simulations with isotropic boundary energy shows the distributions to differ in two regions, termed the “ear” and the “tail”.

Summary and Conclusions

- It is shown that the excess small grains in the region of the “ear” are primarily the 3 and 4-sided grains, whereas the excess of large grains in the “tail” region are grains with more than 9 sides. The excesses in the ear and tail regions of the experimental distributions are necessarily balanced by a deficiency in the mid-sized grains with 6-8 sides.

- Five causes are examined to identify the puzzling difference between simulations with isotropic boundary energy and experiments. These are (i) anisotropy of grain boundary energy, (ii) driving forces other than grain boundary energy reduction, (iii) grain boundary grooving, (iv) solute drag and (v) triple junction drag. No single cause is seen to provide an explanation for the observed experimental behavior.

- However, it is speculated that a combination of causes that include the anisotropy of grain boundary energy will be needed to explain the experimental behavior